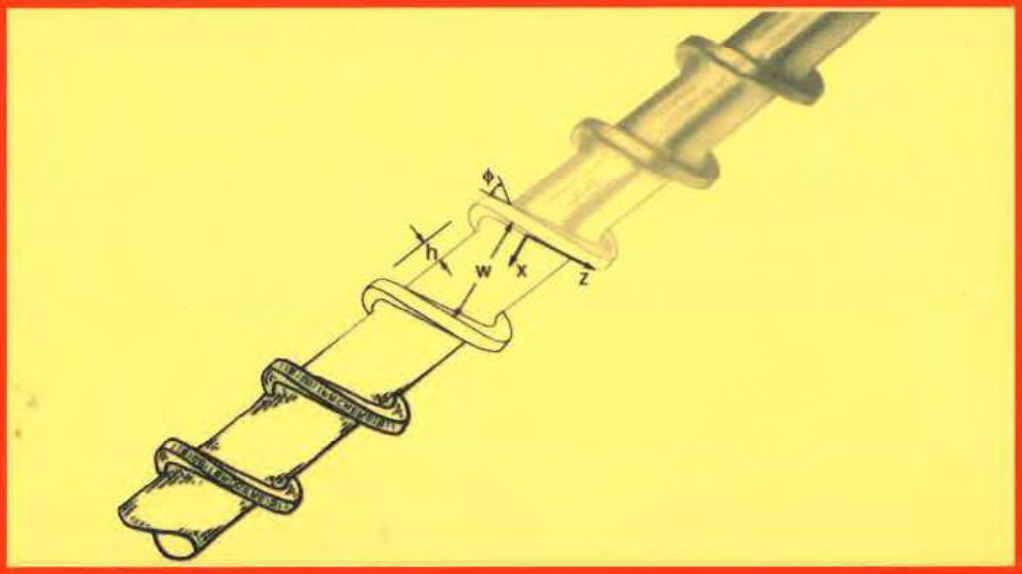
Polymer Processing
Fundamentals

Tim A. Osswald



HANSER

EG_000216510

SPE Books from Hanser Publishers

Belofsky, Plastics: Product Design and Process Engineering
Bernhardt, Computer Aided Engineering for Injection Molding
Brostow/Corneliussen, Failure of Plastics
Chan, Polymer Surface Modification and Characterization
Charrier, Polymeric Materials and ProcessingPlastics, Elastomers and Composites
Del Vecchio, Understanding Design of Experiments: A Primer for Technologists
Ehrig, Plastics Recycling
Ezrin, Plastics Failure Guide
Gordon, Total Quality Process Control for Injection Molding
Gordon/Shaw, Computer Programs for Rheologists
Gruenwald, Plastics: How Structure Determines Properties
Lee, Blow Molding Design Guide
Macosko, Fundamentals of Reaction Injection Molding
Malloy, Plastic Part Design for Injection Molding
Manzione, Applications of Computer Aided Engineering in Injection Molding
Matsuoka, Relaxation Phenomena in Polymers
Menges/Mohren, How to Make Injection Molds
Michaeli, Extrusion Dies for Plastics and Rubber
Michaeli/Greif/Kaufmann/Vossebürger, Training in Plastics Technology
Michaeli/Greif/Kretzschmar/Kaufmann/Bertuleit, Training in Injection Molding
Neuman, Experimental Strategies for Polymer Scientists and Plastics Engineers
O'Brien, Applications of Computer Modeling for Extrusion and Other Continuous Polymer Processes
Osswald, Polymer Processing Fundamentals
Progelhof/Throne, Polymer Engineering Principles
Rauwendaal, Polymer Extrusion
Rees, Mold Engineering
Rosato, Designing with Reinforced Composites
Saechtling, International Plastics Handbook for the Technologist, Engineer and User
Stevenson, Innovation in Polymer Processing
Stoeckhert, Mold-Making Handbook for the Plastics Engineer
Throne, Thermoforming
Tucker, Fundamentals of Computer Modeling for Polymer Processing
Ulrich, Introduction to Industrial Polymers
Wright, Injection/Transfer Molding of Thermosetting Plastics
Wright, Molded Thermosets: A Handbook for Plastics Engineers, Molders and Designers

Tim A. Osswald

Polymer Processing Fundamentals

HANSER

Hanser Publishers, Munich

Hanser Gardner Publications, Inc., Cincinnati

EG_000216511

The Author:
Tim A. Osswald, University of Wisconsin-Madison, Polymer Research Group,
Department of Mechanical Engineering, Madison, WI 53706, USA

Distributed in the USA and in Canada by
Hanser/Gardner Publications, Inc.
6915 Valley Avenue, Cincinnati, Ohio 45244-3029, USA
Fax: (513) 527-8950
Phone: (513) 527-8977 or 1-800-950-8977
Internet: http://www.hansergardner.com

Distributed in all other countries by
Carl Hanser Verlag
Postfach 86 04 20, 81631 München, Germany
Fax: +49 (89) 98 12 64

The use of general descriptive names, trademarks, etc., in this publication, even if the former are not especially identified, is not to be taken as a sign that such names, as understood by the Trade Marks and Merchandise Marks Act, may accordingly be used freely by anyone.

While the advice and information in this book are believed to be true and accurate at the date of going to press, neither the authors nor the editors nor the publisher can accept any legal responsibility for any errors or omissions that may be made. The publisher makes no warranty, express or implied, with respect to the material contained herein.

Library of Congress Cataloging-in-Publication Data
Osswald, Tim A.
Polymer processing fundamentals / Tim A. Osswald.
p. cm.
Includes bibliographical references and index.
ISBN 1-56990-262-3 (pbk.)
1. Plastics. I. Title.
TP1120.D85 1998
668.4–cc21 98-33644

Die Deutsche Bibliothek – CIP-Einheitsaufnahme
Osswald, Tim A.
Polymer processing fundamentals / Tim A. Osswald. – Munich :
Hanser ; Cincinnati : Hanser/Gardner, 1998
ISBN 3-446-19571-8

All rights reserved. No part of this book may be reproduced or transmitted in any form or by any means, electronic or mechanical, including photocopying or by any information storage and retrieval system, without permission in writing from the publisher.

© Carl Hanser Verlag, Munich 1998
Camera-ready copy prepared by the author
Printed and bound in Germany by Druckhaus "Thomas Müntzer", Bad Langensalza

In loving memory of Max Robert Osswald

EG_000216512

ClearCorrect Exhibit 1038, Page 3 of 125

Foreword

The Society of Plastics Engineers is pleased to sponsor and endorse "Polymer Processing Fundamentals" by Tim Osswald. This volume is extremely well written and structured. The comprehensive text makes it an excellent resource for students and engineers. The author's writing style and knowledge of the subject matter have resulted in a competent, well-balanced presentation.

SPE, through its Technical Volumes Committee, has long sponsored books on various aspects of plastics. Its involvement has ranged from identification of needed volumes and recruitment of authors to peer review and approval and publication of new books.

Technical competence pervades all SPE activities, not only in the publication of the books, but also in other areas such as sponsorship of technical conferences and educational programs. In addition, the Society publishes periodicals including *Plastics Engineering, Polymer Engineering and Science, The Journal of Injection Molding Technology, Journal of Vinyl & Additive Technology* and *Polymer Composites* as well as conference proceedings and other publications, all of which are subject to rigorous technical review procedures.

The resource of some 38,000 practicing plastics engineers, scientists, and technologists has made SPE the largest organization of its type worldwide. Further information is available from the Society at 14 Fairfield Drive, Brookfield, Connecticut 06804, USA.

Michael R. Cappelletti
Executive Director
Society of Plastics Engineers

Technical Volumes Committee
Robert C. Portnoy, Chairperson
Exxon Chemical Company

Dan Weissman, Reviewer
Schmalbach Lubeca

EG_000216513

Preface

This book provides some background on polymer processing to engineering students and practicing engineers. It is written at two levels: an introductory level for students and engineers unfamiliar with polymer processing, and a more advanced level for more in-depth material. The more advanced material is shaded to distinguished it from the introductory level. The book presents enough information so that, with their fluids and heat transfer background, engineers can understand and solve polymer processing problems.

Polymer Processing Fundamentals is based on lecture notes from a five-week polymer processing laboratory course taught at the University of Wisconsin-Madison. The introductory level of this book is currently being used in this course.

The first three chapters cover general topics such as historical background, molecular structure of polymers, thermal properties of polymers, mechanical behavior of polymers, and polymer rheology. Chapters 4 through 8 cover the most important polymer processes. Chapter 4 is dedicated to extrusion, Chapter 5 to mixing and Chapter 6 to injection molding. Secondary shaping such as film blowing, film casting, blow molding, and thermoforming is detailed in Chapter 7. The last chapter covers other processes such as calendering, coating, compression molding, foaming, and rotational molding. Laboratory exercises on extrusion, injection molding, blow molding, thermoforming, and film blowing are presented at the end of the book.

I cannot possibly acknowledge everyone who helped in the preparation of this manuscript. First, I would like to thank all the students of my polymer processing course who, in the past few years, have endured my experimenting with new ideas. I am also grateful to my polymer processing colleagues who taught the course before me: Ronald L. Daggett, a true polymer processing pioneer, who had enough vision to include plastics and plastics processing in the mechanical engineering curriculum at the University of Wisconsin-Madison in 1946; the late Lew Erwin, who greatly contributed to the field of mixing, and who continued Daggett's quest; and Jeroen Rietveld who completely renovated the polymer processing laboratories in the early 90s and developed the laboratories presented in this book. Special thanks are due to A. Jeffrey Giacomin for reviewing and proofreading the entire manuscript, and for serving as a sounding board during the preparation of the book. Bruce Davis, Paul Gramann, Antoine Rios, and Richard Theriault I thank for proofreading and giving constructive suggestions. I thank Daniel Feiler for preparing the camera-ready manuscript and for the superb job in drawing most of the figures. Daniel Feiler and Lynda Litzkow are acknowledged for helping with the cover design. I am grateful to Lian Zhao for developing the film blowing laboratory, and to Maria del Pilar Noriega of the ICIPC in Medellin, Colombia, for the extrusion laboratory data. Special thanks to Wolfgang Cohnen for the photograph of Nestles Canyon used in Chapter 3. I am grateful to Wolfgang Glenz, Ed Immergut, Martha Kürzl, and Christine Strohm of Hanser Publishers for their support throughout the book's development, and to Thea Teich for copyediting the final manuscript. Above all, I thank my wife Diane, and my children Palitos and Rudi for everything.

Tim A. Osswald

EG_000216514

ClearCorrect Exhibit 1038, Page 5 of 125

Table of Contents

1 Introduction to Polymers 1

1.1 Historical Background 1
1.2 General Properties 3
1.3 Macromolecular Structure of Polymers 7
1.4 Molecular Weight 9
1.5 Arrangement of Polymer Molecules 11
1.5.1 Thermoplastic Polymers 11
1.5.2 Amorphous Thermoplastics 11
1.5.3 Semi-Crystalline Thermoplastics 12
1.5.4 Thermosets 13
1.6 Copolymers and Polymer Blends 14
1.7 Polymer Additives 15
1.7.1 Plasticizers 15
1.7.2 Flame Retardants 15
1.7.3 Stabilizers 16
1.7.4 Antistatic Agents 16
1.7.5 Fillers 16
1.7.6 Blowing Agents 17
Examples 17
Problems 18
References 18

2 Mechanical Behavior of Polymers 19

2.1 Viscoelastic Behavior of Polymers 19
2.1.1 Stress Relaxation 19
2.1.2 Time-Temperature Superposition 20
2.2 The Short-Term Tensile Test 22
2.2.1 Elastomers 23
2.2.2 Thermoplastic Polymers 25
2.3 Long-Term Tests 26
2.3.1 Isochronous and Isometric Creep Plots 27
2.3.2 Creep Rupture 29
2.4 Dynamic Mechanical Tests 29
2.5 Mechanical Behavior of Filled and Reinforced Polymers 32
2.6 Impact Strength 36
2.7 Fatigue 38
2.8 Weathering 40
Examples 41
Problems 43

EG_000216515

ClearCorrect Exhibit 1038, Page 6 of 125

References....45

3 Rheology of Polymer Melts....47

3.1 Introduction to Rheology....47
3.1.1 Shear Thinning Behavior of Polymers....48
3.1.2 Normal Stresses in Shear Flow....52
3.1.3 Deborah Number....54
3.1.4 Rheology of Curing Thermosets....56
3.1.5 Suspension Rheology....57
3.2 Rheometry....59
3.2.1 The Melt Flow Indexer....60
3.2.2 The Capillary Viscometer....60
3.2.3 The Cone-and-Plate Rheometer....63
Examples....64
Problems....65
References....65

4 Extrusion....67

4.1 The Plasticating Extruder....69
4.1.1 The Solids Conveying Zone....72
4.1.2 The Melting Zone....76
4.1.3 The Metering Zone....79
4.2 Extrusion Dies....81
4.2.1 Sheeting Dies....82
4.2.2 Tubular Dies....84
Examples....85
Problems....91
References....93

5 Mixing....95

5.1 Distributive Mixing....95
5.1.1 Effect of Orientation....96
5.2 Dispersive Mixing....99
5.2.1 Break-Up of Particulate Agglomerates....99
5.2.2 Break-Up of Fluid Droplets....102
5.3 Mixing Devices....104
5.3.1 Banbury Mixer....105
5.3.2 Mixing in Single Screw Extruders....106
5.3.3 Static Mixers....109
5.3.4 Cokneader....110
5.3.5 Twin Screw Extruders....111
Examples....112
Problems....114

References....115

6 Injection Molding....117

6.1 The Injection Molding Cycle....118
6.2 The Injection Molding Machine....120
6.2.1 The Plasticating and Injection Unit....126
6.2.2 The Clamping Unit....127
6.2.3 The Mold Cavity....128
6.3 Related Injection Molding Processes....131
6.4 Computer Simulation in Injection Molding....132
Examples....133
Problems....137
References....139

7 Secondary Shaping....141

7.1 Fiber Spinning....141
7.2 Film Production....143
7.2.1 Cast Film Extrusion....143
7.2.2 Film Blowing....145
7.3 Blow Molding....148
7.3.1 Extrusion Blow Molding....149
7.3.2 Injection Blow Molding....151
Examples....155
Problems....157
References....157

8 Other Important Polymer Processes....159

8.1 Calendering....159
8.2 Coating....163
8.3 Processing Reactive Polymers....167
8.4 Compression Molding....171
8.5 Foaming....175
8.6 Rotational Molding....176
Examples....177
Problems....177
References....178

EG_000216516

ClearCorrect Exhibit 1038, Page 7 of 125

Appendix 181

A1 Extrusion Laboratory 183

A1.1 Objective 183
A1.2 Laboratory Equipment 183
A1.2.1 Extruder 183
A1.2.2 Material 184
A1.2.3 Utilities 184
A1.3 Experimental Procedure 185

A2 Injection Molding Laboratory 187

A2.1 Objective 187
A2.2 Laboratory Equipment 188
A2.2.1 Injection Molder 188
A2.2.2 Utilities 189
A2.3 Experimental Procedure 189

A3 Blow Molding Laboratory 195

A3.1 Objective 195
A3.2 Laboratory Equipment 195
A3.2.1 Blow Molder 195
A3.2.2 Utilities 195
A3.3 Experimental Procedure 196

A4 Thermoforming Laboratory 201

A4.1 Objective 201
A4.2 Laboratory Equipment 201
A4.2.1 Thermoforming Machine 201
A4.2.2 Utilities 203
A4.3 Experimental Procedure 203

A5 Film Blowing Laboratory 207

A5.1 Objective 207
A5.2 Laboratory Equipment 207
A5.2.2 Utilities 207
A5.3 Experimental Procedure 209

A6 Transport Phenomena Equations 213

A7 Properties Table 217

Subject Index 227

Biography 231

EG_000216517

ClearCorrect Exhibit 1038, Page 8 of 125

1 Introduction to Polymers

As the word suggests, polymers* are materials composed of molecules of high molecular weight. These large molecules are generally called *macromolecules*. The unique material properties of polymers and versatility of processing methods are attributed to their molecular structure. The ease with which polymers and *plastics* ** are processed makes them, for many applications, the most sought after materials today. Because of their low density and their ability to be shaped and molded at relatively low temperatures, compared to traditional materials such as metals, plastics and polymers are the material of choice when integrating several parts into a single component—a design step usually called *part consolidation*. In fact, parts and components, traditionally made of wood, metal, ceramics, or glass, are frequently redesigned with plastics.

1.1 Historical Background

Natural polymeric materials such as rubber have been in use for thousands of years. Natural rubber also known as *caoutchouc* (crying trees) has been used by South American Indians in the manufacture of waterproof containers, shoes, torches, and squeeze bulb pumps. The first Spanish explorers of Haiti and Mexico reported that natives played games on clay courts with rubber balls [1]. Rubber trees were first mentioned in *De Orbe Novo*, originally published in Latin, by Pietro Martire d'Anghiera in 1516. The French explorer and mathematician Charles Maria de la Condamine, who was sent to Peru by the French *Academie des Sciences*, brought caoutchouc from South America to Europe in the 1740s. In his report [2] he mentions several rubber items made by native South Americans including a pistonless pump composed of a rubber pear with a hole in the bottom. He points out that the most remarkable property of natural rubber is its great elasticity.

The first chemical investigations on *gummi elasticum* were published by the Frenchman Macquer in 1761. However, it was not until the 20th century that the molecular architecture of polymers was well understood. Soon after its introduction to Europe, various uses were found for natural rubber. Gossart manufactured the first polymer tubes in 1768 by wrapping rubber sheets around glass pipes. During the same time period small rubber blocks where introduced to erase lead pencil marks from paper. In fact, the word *rubber* originates from this specific application—*rubbing*.

These new materials slowly evolved from novelty status as a result of new applications and processing equipment. Although the screw press, the predecessor of today's compression molding press, was patented in 1818 by McPherson Smith [3], the first documented *polymer processing* machinery dates to 1820 when Thomas Hancock invented a rubber masticator. This masticator, consisting of a toothed rotor in a toothed cylindrical

* From the Greek, *poli* which means many, and *meros* which means parts.

** The term plastics describes the compound of a polymer with one or more additives.

EG_000216518

ClearCorrect Exhibit 1038, Page 9 of 125

cavity [4], was used to reclaim rubber scraps which resulted from the manual manufacturing process of elastic straps, perhaps the first recycling effort. In 1833 the development of the vulcanization process by Charles Goodyear [5] greatly enhanced the properties of natural rubber, and in 1836 Edwin M. Chaffee invented the two roll steam heated mill, the predecessor of the calender, for continuously mixing additives into rubber for the manufacture of rubber-coated textiles and leathers. As early as 1845, presses and dies were used to mold buttons, jewelry, dominoes, and other novelties out of shellac and gutta-percha. *Gutta-percha* (rubber clump), a gum found in trees similar to rubber, became the first wire insulation and was used for ocean cable insulation for many years.

The ram-type extruder was invented by Henry Bewley and Richard Brooman in 1845. The first *polymer processing* screw extruder, the most influential equipment in polymer processing, was patented by an Englishman named Mathew Gray in 1879 for the purpose of wire coating. However, the screw pump is attributed to Archimedes, and the actual invention of the screw extruder by A.G. DeWolfe of the U.S. dates back to the early 1860s.

Cellulose nitrate plasticized by camphor, possibly the first thermoplastic, was patented by Isaiah and John Hyatt in 1870. Based on experience from metal injection molding, the Hyatt brothers built and patented the first injection molding machine in 1872 to mold cellulose materials [6].

With the mass production of rubber, gutta-percha, cellulose, and shellac articles during the height of the industrial revolution, the polymer processing industry after 1870 saw the invention and development of internal kneading and mixing machines for the processing and preparation of raw materials [7]. A notable invention was the Banbury mixer, developed by Fernley Banbury in 1916. This mixer, with some modifications, is still used for rubber compounding.

Bakelite, developed by Leo Baekeland in 1907, was the first synthetically developed polymer. Bakelite, also known as phenolic, is a thermoset resin that reacts by condensation polymerization occurring when phenol and formaldehyde are mixed and heated.

In 1924, Hermann Staudinger proposed a model that described polymers as linear molecular chains. Once this model was accepted by other scientists, the concept used to synthesize new materials was realized. In 1927 cellulose acetate and polyvinyl chloride (PVC) [8] were developed. Because of its higher wear resistance, polyvinyl chloride replaced shellac for phonograph records in the early 1930s. Wallace Carothers pioneered condensation polymers such as polyesters and polyamides. It was not until this point that the scientific world was finally convinced of the validity of Staudinger's work. Polyamides, first called Nylon, were set into production in 1938. Polyvinyl acetate, acrylic polymers, polystyrene (PS), polyurethanes, and melamine were also developed in the 1930s [9].

The first single screw extruder designed for the processing of thermoplastic polymers was built circa 1935 at the Paul Troester Maschinenfabrik [10]. Around that same time period, Roberto Colombo developed a twin screw extruder for thermoplastics.

World War II and the post-war years saw accelerated development of new polymeric materials. Polyethylene (PE), polytetrafluoroethylene, epoxies, and acrylonitrile-butadiene-styrene (ABS) were developed in the 1940s, and linear polyethylene, polypropylene (PP), polyacetal, polyethylene terephthalate (PET), polycarbonate (PC), and many more

materials came in the 1950s. The 1970s saw the development of new polymers such as polyphenylene sulfide and the 1980s, liquid crystalline polymers.

Developing and synthesizing new polymeric materials has become increasingly expensive and difficult. Developing new engineering materials by blending or mixing two or more polymers or by modifying existing ones with plasticizers is now widely accepted.

The world's yearly production of polymer resins has experienced steady growth since the turn of the century, with growth predicted well into the 21st century. Figure 1.1 [11] presents the world's yearly polymer production in millions of tons. In developed countries, the growth in annual polymer production has decreased recently. However, developing countries in South America and Asia are now starting to experience tremendous growth.

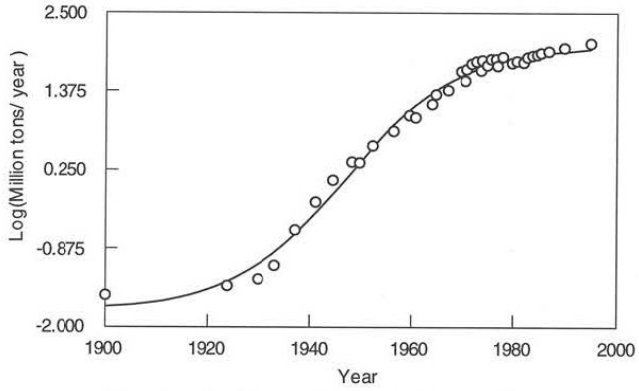


Figure 1.1 World yearly plastics production since 1900

Of the more than 31 million tons of polymers produced in the U.S. in 1993, 90% were thermoplastics. Figure 1.2 breaks the U.S. polymer production into major polymer categories, including polyethylenes, polypropylene, polystyrene, polyvinyl chloride, and thermosets. Polyethylenes are by far the most widely used polymeric material, accounting for 41% of the U.S. plastic production.

1.2 General Properties

Any plastic resin can be categorized as either a thermoplastic or thermoset. Thermoplastics are those polymers that solidify as they cool, restricting the motion of the long molecules. When heated, these materials regain the ability to "flow," as the molecules can slide past each other easily. Thermoplastic polymers further are divided into two classes: amorphous and semi-crystalline polymers.

EG_000216519

ClearCorrect Exhibit 1038, Page 10 of 125

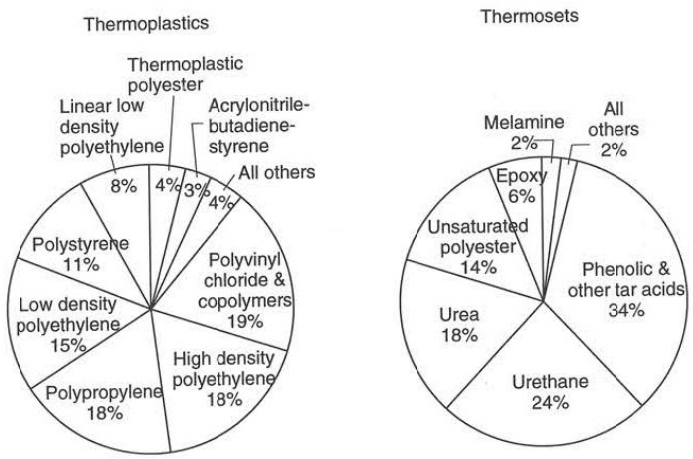


Figure 1.2 Break down of U.S. polymer production into major polymer categories
Source: SPI Committee on Resin Statistics as compiled by Ernst & Young

Amorphous thermoplastics have molecules that remain disorderly as they cool, leading to a material with a random molecular structure. An amorphous polymer solidifies, or vitrifies, as it cools below its glass transition temperature, T_g. Semi-crystalline thermoplastics, on the other hand, solidify with a certain order in their molecular structure. Hence, as they cool, they harden when the molecules arrange in a regular order below what is usually called the melting temperature, T_m. The molecules in semi-crystalline polymers not ordered remain in amorphous regions. These regions within the semi-crystalline domains solidify at the glass transition temperature. Most semi-crystalline polymers have a glass transition temperature below the ice point, and, behave at room temperature similarly to rubbery or leathery materials. Table 1.1 presents the most common amorphous and semi-crystalline thermoplastics with some of their applications.

On the other hand, thermosetting polymers solidify by a chemical cure. Here, the long macromolecules crosslink during cure, resulting in a network. The original molecules can no longer slide past each other. These networks prevent "flow" even after re-heating. The high density of crosslinking between the molecules makes thermosetting materials stiff and brittle. Thermosets also exhibit glass transition temperatures which sometimes exceed thermal degradation temperatures. Some of the most common thermosets and their applications are also found in Table 1.1.

Compared to thermosets, elastomers are only slightly crosslinked, which permits almost full moleculer extension. However, the links across the molecules hinder them from sliding past each other, making even large deformations reversible. One common characteristic of elastomeric materials is that the glass transition temperature is much lower than room temperature. Table 1.1 lists the most common elastomers with some of their applications.

Table 1.1 Common Polymers and Some of Their Applications

Polymer	Some Applications
	Thermoplastics
Amorphous	
Polystyrene	Mass-produced transparent articles, packaging, insulation (foamed)
Polymethyl methacrylate	Skylights, airplane windows, lenses, stop lights
Polycarbonate	Helmets, hockey masks, blinker lights, head lights
Unplasticized polyvinyl chloride	Tubes, window frames, siding, bottles, packaging
Plasticized polyvinyl chloride	Shoes, hoses, calendered films and sheets (floors and upholstery)
Semi-crystalline	
High density polyethylene	Milk and soap bottles, mass produced household goods
Low density polyethylene	Mass produced household goods, grocery bags
Polypropylene	Housings for electric appliances, auto battery cases
Polytetrafluoroethylene	Coating of cooking pans, lubricant-free bearings
Polyamide	Gears, bolts, skate wheels, pipes, fishing line, textiles, ropes
	Thermosets
Epoxy	Adhesive, matrix in fiber-reinforced composite parts
Melamine	Decorative heat-resistant surfaces for kitchens and furniture, dishes
Phenolics	Heat-resistant handles for pans, irons and toasters, electric outlets
Unsaturated polyester	Sinks and tubs, automotive body panels (with glass fiber)
	Elastomers
Polybutadiene	Automotive tires, golf ball skin
Ethylene propylene rubber	Automotive radiator hoses and window seals, roof covering
Natural rubber (polyisoprene)	Automotive tires, engine mounts
Polyurethane elastomer	Roller skate wheels, automotive seats (foamed), shoe soles (foamed)
Silicone rubber	Seals, flexible hoses for medical applications
Styrene butadiene rubber	Automotive tire treads

As mentioned earlier, there are thousands of grades of polymers available to the design engineer. These cover a wide range of properties, from soft to hard, ductile to brittle, and weak to tough. Figure 1.3 shows this range by plotting important average properties for selected polymers. The abbreviations used in Fig. 1.3 are defined in Table 1.2. The values for each material in Fig. 1.3 are representative averages.

The relatively low stiffness of polymeric materials is attributed to their molecular structure, which allows relative movement with ease while under stress. However, the strength and stiffness of individual polymer chains are much higher than the measured properties of the bulk. For example, polyethylene whose molecules have a theoretical stiffness of 300,000 MPa, has a bulk stiffness of only 1,000 MPa [12,13]. By introducing high molecular orientation, the stiffness and strength of a polymer can be substantially increased. In the case of *ultra-drawn, ultra high molecular weight high density polyethylene,* UHMHDPE, fibers can exceed a stiffness 200,000 MPa [13].

EG_000216520

ClearCorrect Exhibit 1038, Page 11 of 125

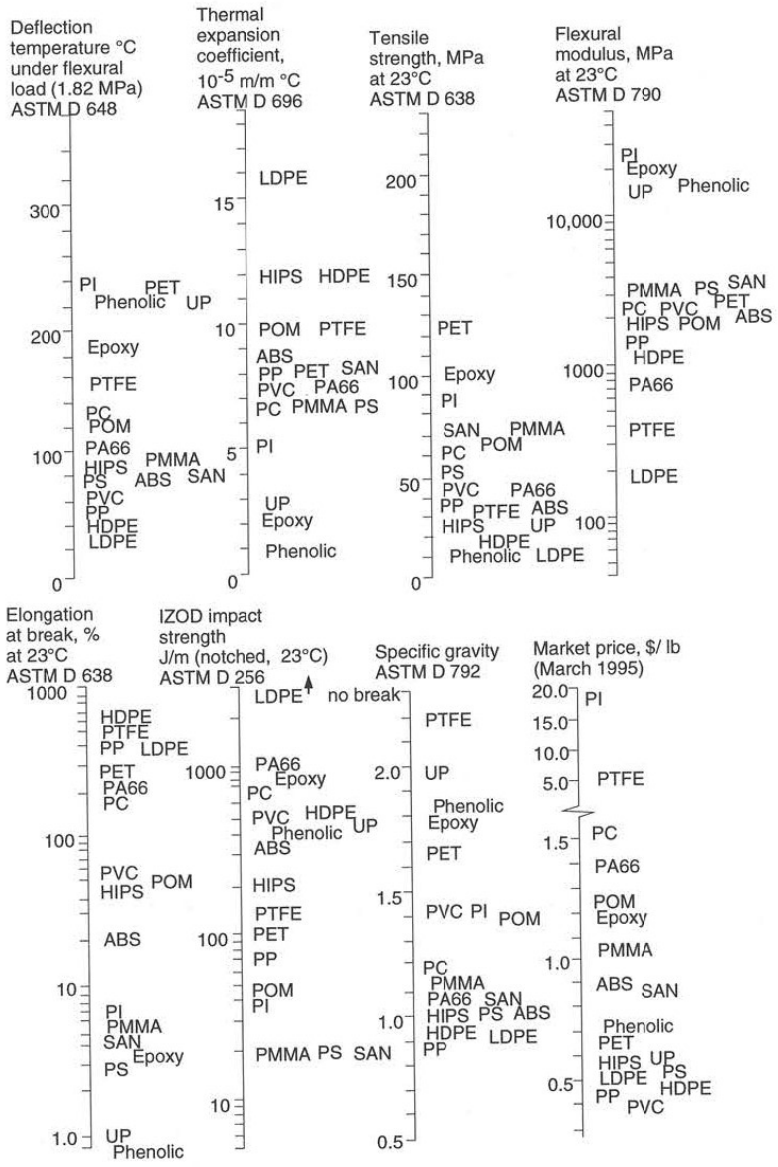


Figure 1.3 Average properties for common polymers

Table 1.2 Abbreviation of Common Polymers

Polymer	ASTM D1600-93 abbreviation
Acrylonitrile-butadiene-styrene	ABS
Epoxy	EP
High density polyethylene	HDPE
Impact resistant polystyrene	IPS (HIPS)
Low density polyethylene	LDPE
Phenol-formaldehyde (Phenolic)	PF
Polyacetal (polyoxymethylene)	POM
Polyamide 66	PA 66
Polycarbonate	PC
Polyethylene terephthalate	PET
Polyimide	PI
Polymethyl methacrylate	PMMA
Polypropylene	PP
Polystyrene	PS
Polytetrafluoroethylene	PTFE
Polyvinyl chloride	PVC
Styrene-acrylonitrile copolymer	SAN
Unsaturated polyester	UP

1.3 Macromolecular Structure of Polymers

Polymers are macromolecular structures generated synthetically or through natural processes. Cotton, silk, natural rubber, ivory, amber and wood are a few materials that occur naturally with an organic macromolecular structure, whereas natural inorganic materials include quartz and glass. The other class of organic materials with a macromolecular structure are synthetic polymers, which are generated through addition polymerization or condensation polymerization.

In addition polymerization, monomers are added to each other by breaking the double-bonds that exist between carbon atoms, allowing them to link to neighboring carbon atoms to form long chains. The simplest example is the addition of ethylene monomers, schematically shown in Fig. 1.4, to form polyethylene molecules as shown in Fig. 1.5. The schematic shown in Fig. 1.5 can also be written symbolically as shown in Fig. 1.6. Here, the subscript n represents the number of repeat units which determines the molecular weight of a polymer. The number of repeat units is more commonly referred to as the degree of polymerization.

EG_000216521

ClearCorrect Exhibit 1038, Page 12 of 125

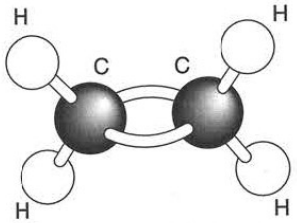


Figure 1.4 Schematic representation of an ethylene monomer

Another technique for producing macromolecular materials is condensation polymerization. Condensation polymerization occurs when two components with end-groups that react with each other are mixed. When they are stoichiometric, these end-groups react, linking them to chains and leaving a by-product such as water. A common polymer made by condensation polymerization is polyamide where diamine and diacid groups react to form polyamide and water as shown in Fig. 1.7.

In the molecular level, there are several forces that hold a polymeric material together. The most basic forces are the covalent bonds which hold the polymer backbone together, such as the -C-C- or -C-N- bond.

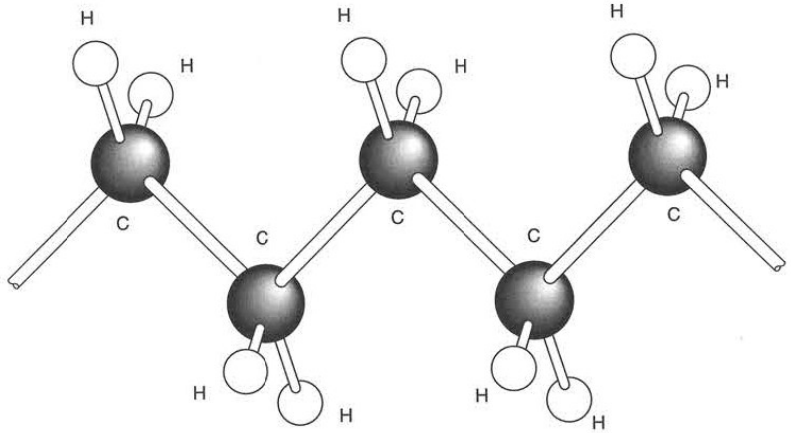


Figure 1.5 A polyethylene molecule

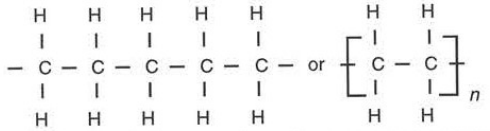


Figure 1.6 Symbolic representation of a polyethylene molecule

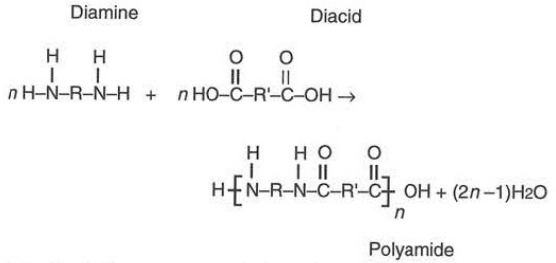


Figure 1.7 Symbolic representation of the condensation polymerization of polyamide

1.4 Molecular Weight

A polymeric material usually consists of polymer chains of various lengths. With the exception of some naturally occurring polymers, most polymers have a molecular weight distribution such as shown in Fig. 1.8 and the molecular weight is described by a set of averages. The properties of polymeric material are strongly linked to the molecular weight of the polymer as shown schematically in Fig. 1.9. A polymer such as polystyrene is stiff and brittle at room temperature with a degree of polymerization of 1,000. However, at a degree of polymerization of 10, polystyrene is sticky and soft at room temperature. The stiffness properties reach an asymptotic maximum, whereas the flow temperature increases with molecular weight. One must find the molecular weight of a polymer that renders ideal mechanical properties, while maintaining flow properties that make it easy to shape the material during manufacturing.

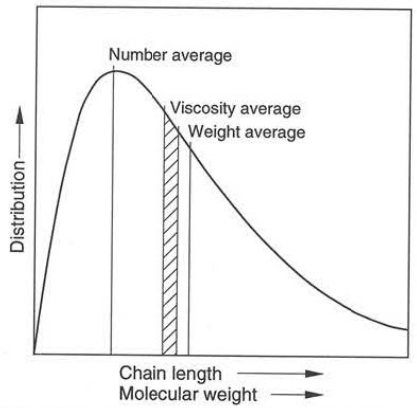


Figure 1.8 Molecular weight distribution of a typical thermoplastic

EG_000216522

ClearCorrect Exhibit 1038, Page 13 of 125

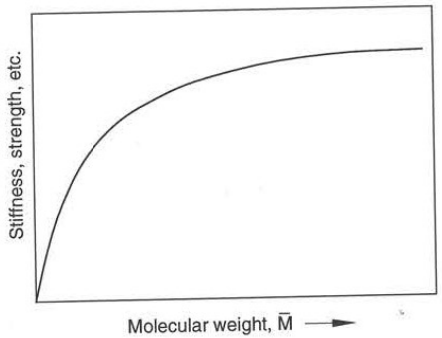


Figure 1.9 Influence of molecular weight on mechanical properties

Polymer chain Branching, which occurs due to irregularities during polymerization, also influences the final structure, crystallinity and properties of the polymeric material. Figure 1.10 shows the molecular architecture of high density, low density and linear low density polyethylenes (LLDPE). The high density polyethylene (HDPE) has between 5 and 10 short branches every 1000 carbon atoms. The low density material (LDPE) has the same number of branches as HDPE; however, they are much longer and are themselves usually branched. The LLDPE has between 10 and 35 short chains every 1000 carbon atoms. Polymer chains with fewer and shorter branches can crystallize more easily resulting in higher density.

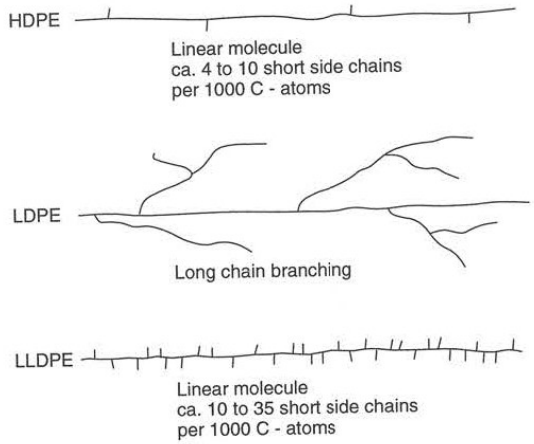


Figure 1.10 Schematic of the molecular structure of different polyethylenes

1.5 Arrangement of Polymer Molecules

Polymeric materials can be categorized as either thermoplastics or thermosets. Thermoplastics can remelt after solidification, and thermosets solidify via a chemical reaction that causes polymer molecules to crosslink. These crosslinked materials cannot be remelted after solidification.

As thermoplastic polymers solidify, they take on two different types of structure: amorphous and semi-crystalline. Amorphous polymers are those where the molecules solidify in a random arrangement, whereas the molecules in semi-crystalline polymers align with their neighbors, forming regions with a three-dimensional order.

1.5.1 Thermoplastic Polymers

The formation of macromolecules from monomers occurs if there are unsaturated carbon atoms (carbon atoms connected with double or triple bonds), or if there are monomers with reactive end-groups. For example, in an ethylene monomer a double bond is split which frees two valence electrons per monomer and leads to the formation of a macromolecule such as polyethylene. This process is called polymerization. Similarly, two complementing monomers (R and R') that each posess two reactive end groups (bifunctional) can react with each other, also leading to the formation of a polymer chain.

1.5.2 Amorphous Thermoplastics

Amorphous thermoplastics, with their randomly arranged molecular structure, are analogous to spaghetti. Because of their structure, the characteristic size of the largest ordered region is length of a carbon-carbon bond. This dimension is much smaller than the wavelength of visible light and so generally makes amorphous thermoplastics very clear, and in most cases close to transparent.

Figure 1.11 [14] shows the shear modulus, G', versus temperature for polystyrene, one of the most common amorphous thermoplastics. The figure, which was obtained through a dynamic-mechanical test, shows two general regions: one where the modulus appears fairly constant, and one where the modulus drops significantly with increasing temperature. With decreasing temperatures, the material enters the glassy region where the slope of the modulus approaches zero. At high temperatures, the modulus is negligible and the material is soft enough to flow. Although there is no clear transition between "solid" and "liquid," the temperature dividing the two states in an amorphous thermoplastic is called the *glass transition temperature* T_g. For the polystyrene in Fig. 1.11, the glass transition temperature is about 110 °C. Although data is usually presented in the form shown in Fig. 1.11, the curve shown in the figure was measured at a constant frequency. If the test frequency is increased—reducing the time scale—the curve shifts to the right, because higher temperatures are required to achieve molecular motion at the new frequency.

EG_000216523

ClearCorrect Exhibit 1038, Page 14 of 125

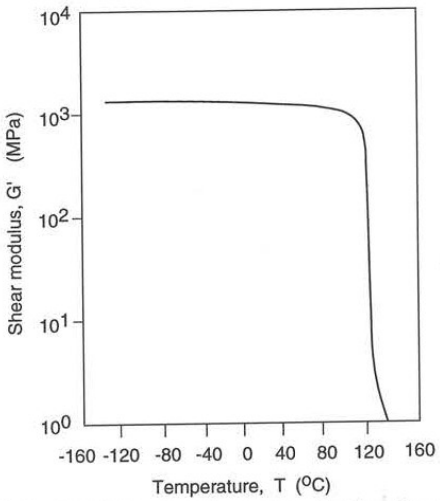


Figure 1.11 Shear modulus of polystyrene as a function of temperature

1.5.3 Semi-Crystalline Thermoplastics

The molecules in semi-crystalline thermoplastic polymers align in an ordered crystal structure as shown for polyethylene in Fig. 1.12. The schematic shows the general structure and hierarchical arrangement in semi-crystalline materials. The crystalline structure is part of a *lamellar crystal* which in turn forms the *spherulites*. The sperulitic structure is the largest domain with a specific order and has a characteristic size of 50 to 500 μm. This is much larger than the wavelength of visible light, making semi-crystalline materials translucent, not transparent.

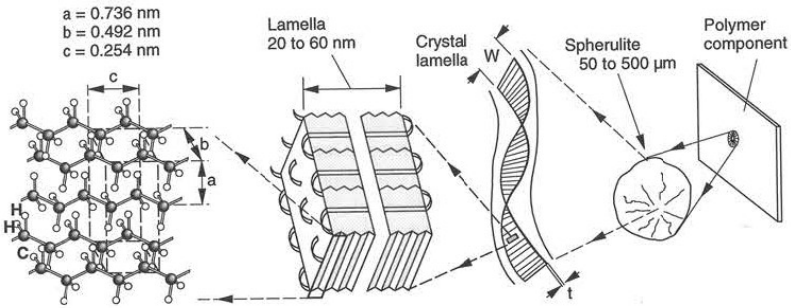


Figure 1.12 Schematic representation of the general molecular structure and arrangement of typical semi-crystalline materials

However, the crystalline regions are tiny with molecular chains comprised of both crystalline and amorphous regions. The degree of crystallinity in a typical thermoplastic varies from grade to grade. For example, in polyethylene, the degree of crystallinity depends on the branching and the cooling rate. LDPE with its long branches (Fig.1.10) can only crystallize to about 40 to 50%, whereas a HDPE crystallizes to up to 80%. The density and strength of semi-crystalline thermoplastics increase with the degree of crystallinity.

Figure 1.13 [14] shows the dynamic shear modulus versus temperature for a HDPE, the most common semi-crystalline thermoplastic. Again, this curve presents data measured at one test frequency. The figure clearly shows two distinct transitions: one at about -110 °C, the *glass transition temperature* and another near 140 °C, the *melting temperature*. Above the melting temperature, the shear modulus is negligible and the material flows. Crystalline arrangement begins to develop as the temperature dips below the melting point. Between the melting and glass transition temperatures, the material behavior is leathery. As the temperature dips below the glass transition temperature, the amorphous regions within the semi-crystalline structure solidify, forming a glassy, stiff, and sometimes brittle polymer.

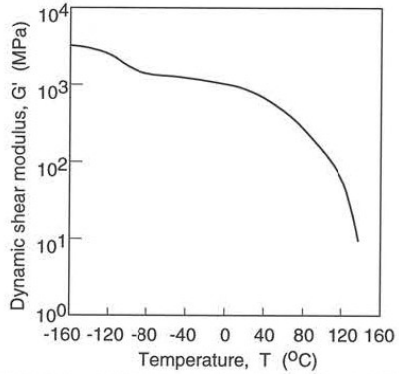


Figure 1.13 Shear modulus of HDPE versus temperature

1.5.4 Thermosets and Crosslinked Elastomers

Thermosets and some elastomers are polymeric materials that can crosslink. The crosslinking causes the material to resist heat after solidification. A more in-depth explanation of the crosslinking chemical reaction that occurs during solidification is given in section 8.3.

Crosslinking is usually a result of double bonds breaking, allowing molecules to link with their neighbors. One of the oldest thermosetting polymers is phenol-formaldehyde or phenolic. Figure 1.14 shows the chemical symbol representation of the reaction. The phenol and formaldehyde molecules react to create a three-dimensional cross-linked network that is stiff and strong. The by-product of this chemical reaction is water.

EG_000216524

ClearCorrect Exhibit 1038, Page 15 of 125

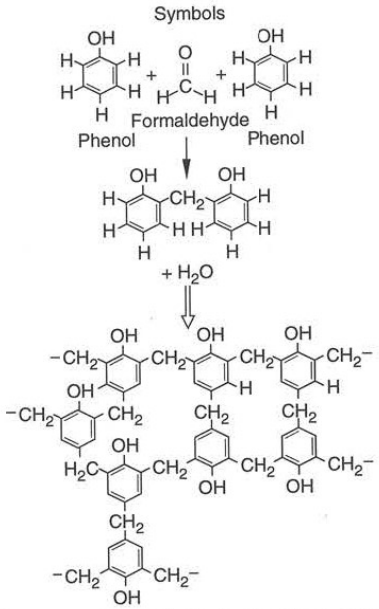


Figure 1.14 Symbolic representation of the condensation polymerization of phenol-formaldehyde resins

1.6 Copolymers and Polymer Blends

Copolymers are polymeric chains of materials with two or more monomer types. A copolymer that is composed of two monomer types is called a *bipolymer*, and one formed from three different monomer groups is called a *terpolymer*. Depending on how the different monomers are arranged in the polymer chain, distinguishes them as *random, alternating, block,* or *graft* copolymers. These copolymer types are schematically represented in Fig. 1.15.

A widely used copolymer is high impact polystyrene (PS-HI), formed by grafting polystyrene to polybutadiene. If styrene and butadiene are randomly copolymerized, the resulting material is an elastomer called styrene-butadiene-rubber (SBR). Another classic example of copolymerization is the terpolymer acrylonitrile-butadiene-styrene (ABS).

Polymer blends belong to another family of polymeric materials which are made by mixing or blending two or more polymers to enhance the physical properties of each individual component. Common polymer blends include PP+PC, PVC+ABS, PE+PTFE, and ABS+PC.

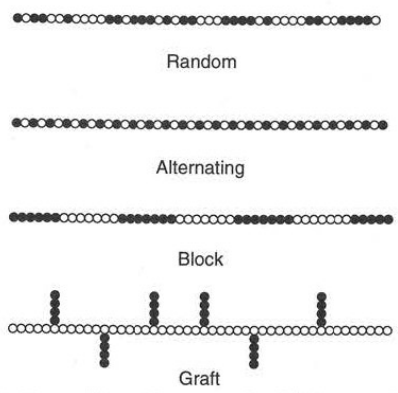


Figure1.15 Schematic representation of different copolymers

1.7 Polymer Additives

A polymer seldom is sold as a pure material. More often a polymer contains several additives to aid during processing, add color, or enhance the mechanical properties.

1.7.1 Plasticizers

Solvents, commonly called plasticizers, are sometimes mixed into a polymer to dramatically alter its rheological or mechanical properties. Plasticizers are used as processing aids since they have the same effect as raising the temperature of the material. The resulting lowered viscosities reduce the risk of thermal degradation during processing. For example, cellulose nitrite thermally degrades if it is processed without a plasticizer.

Plasticizers are more commonly used to alter a polymer's mechanical properties such as stiffness, toughness, and strength. For example, adding a plasticizer such as dioctylphthalate (DOP) to PVC can reduce its stiffness by three orders of magnitude and can lower its glass transition temperature by 35 °C. In fact, highly plasticized PVC is rubbery at room temperature.

1.7.2 Flame Retardants

Since polymers are organic materials, most of them are flammable. The flammability of polymers has always been a serious technical problem. However, some additives that contain halogens, such as bromine or chlorine or phosphorous, reduce the possibility of either ignition within a polymer component or once ignited, flame spread. Bromine is more effective flame retardant than chlorine.

EG_000216525

ClearCorrect Exhibit 1038, Page 16 of 125

1.7.3 Stabilizers

The combination of heat and oxygen can result in thermal degradation in a polymer. Heat or energy produce free radicals which react with oxygen to form carbonyl compounds, giving rise to yellow or brown discolorations in the final product.

Thermal degradation can be suppressed by adding stabilizers, such as antioxidants or peroxide decomposers. These additives do not eliminate thermal degradation but slow it down. Once the stabilizer has been consumed by reaction with oxygen, the polymer is no longer protected against thermal degradation.

Polyvinyl chloride is probably the polymer most vulnerable to thermal degradation. In polyvinyl chloride, scission of the C-Cl bond occurs in the weakest point of the molecule. The chlorine radicals react with their nearest CH group, forming HCl and creating new weak C-Cl bonds. A stabilizer must therefore be used to neutralize HCl and stop the autocatalytic reaction, as well as preventing corrosion of processing equipment.

1.7.4 Antistatic Agents

Since polymers have such low electrical conductivity, they can easily build-up electric charges. The amount of charge build-up is controlled by the rate at which the charge is generated compared to the charge decay. The rate of charge generation at the surface of the component can be reduced by reducing the intimacy of contact, whereas the rate of charge decay is increased through surface conductivity. Hence, a good antistatic agent should be an ionizable additive that allows the charge to migrate to the surface. At the same time it should be creating bridges to the atmosphere through moisture in the surroundings. Typical antistatic agents are nitrogen compounds, such as long chain amines, and amides and polyhydric alcohols.

1.7.5 Fillers

Fillers can be classified three ways: those that reinforce the polymer and improve its mechanical performance; those used to take-up space and so reduce the amount of resin to produce a part – sometimes referred to as *extenders*; and those, less common, that are dispersed through the polymer to improve its electric conductivity.

Polymers that contain fillers that improve its mechanical performance are often referred to as reinforced plastics or *composites*. Composites can be furthermore divided into composites with *high performance* reinforcements, and composites with *low performance* reinforcements. The high performance composites are those where the reinforcement is placed inside the polymer so that optimal mechanical behavior is achieved, such as unidirectional glass fibers in an epoxy resin. High performance composites usually have 50 to 80% reinforcement by volume and usually have a laminated tubular shape containing braided reinforcements. The low performance composites are those where the reinforcement is small enough that it can be well dispersed into the matrix. These materials can be processed the same way as their unreinforced counterparts.

The most common filler used to reinforce polymeric materials is glass fiber. However, wood fiber, which is commonly used as an extender, also increases the stiffness and mechanical performance of some thermoplastics. To improve the bonding between the polymer matrix and the reinforcement, *coupling agents* such as *silanes* and *titanates* are often added.

Extenders, used to reduce the cost of the component, are often particulate fillers. The most common of these are calcium carbonate, silica flour, clay, and wood flour or fiber. As mentioned earlier, some fillers also slightly reinforce the polymer matrix, such as clay, silica flour, and wood fiber. Polymers with extenders often have significantly lower toughness than when unfilled.

1.7.6 Blowing Agents

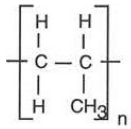
The task of blowing or foaming agents is to produce cellular polymers, also called expanded plastics. The cells can be completely enclosed (closed cell) or can be interconnected (open cell). Polymer foams are produced with densities between 1.6 kg/m^3 and 960 kg/m^3. There are many reasons for using polymer foams, such as their high strength to weight ratio, excellent insulating and acoustic properties, and high energy and vibration absorbing properties.

Polymer foams can be made by mechanically whipping gases into the polymer, or by either chemical or physical means. The basic steps of the foaming process are (1) cell nucleation, (2) expansion or growth of the cells and (3) stabilization of the cells. Cell nucleation occurs when, at a given temperature and pressure, the solubility of a gas is reduced, leading to saturation, and expelling the excess gas to form bubbles. Nucleating agents are used for initial formation of a bubble. The bubble reaches an equilibrium shape when the pressure in the bubble balances the surface tension.

Examples

1.1 Estimate the degree of polymerization of a polypropylene with an average molecular weight of 100,000.

As shown in the diagram below the repeat unit of a polypropylene molecule contains 3 carbon and 6 hydrogen atoms.



From the diagram we can see that each repeat unit's molecular weight is 6(1) + 3(12) = 42. Thus, a molecule with a molecular weight of 100,000 is formed by 100,000/42 = 2381 repeat units.

Problems

1.1 Estimate the degrees of polymerization of a polyethylene with an average molecular weight between 150,000 and 200,000.

EG_000216526

ClearCorrect Exhibit 1038, Page 17 of 125

1.2 What is the maximum possible separation between the ends of a polystyrene molecule with a molecular weight of 160,000 ?

1.3 Write the molecular structure for the following polymers: polyacetal, polycarbonate, polyvinyl chloride, polystyrene, and polytetrafluoroethylene.

References

1. Stern, H.J., *Rubber: Natural and Synthetic*, Maclaren and Sons LDT (1967), London
2. de la Condamine, C.M.,*Relation Abregee D'un Voyage Fait Dans l'interieur de l'Amerique Meridionale*, Academie des Sciences (1745), Paris
3. DuBois, J.H., *Plastics History U.S.A.*, Cahners Publishing Co., Inc. (1972), Boston
4. Tadmor, Z., and C.G. Gogos, *Principles of Polymer Processing*, John Wiley & Sons
5. McPherson, A.T., and A. Klemin, *Engineering Uses of Rubber*, Reinhold Publishing Corporation (1956), New York
6. Sonntag, R., *Kunststoffe* (1985), *75*, 4
7. Herrmann, H., *Kunststoffe* (1985), *75*, 2
8. Regnault, H.V. Liebigs Ann. (1835), 14, 22
9. Ulrich, H., *Introduction to Industrial Polymers*, 2nd Ed., Hanser Publishers (1993), Munich
10. Rauwendaal, C., *Polymer Extrusion*, 2nd Ed., Hanser publishers (1990), Munich
11. Utracki, L.A., *Polym. Eng. Sci.* (1995), 35, 1, 2
12. Termonia, Y., and P. Smith, *High Modulus Polymers*, A.E. Zachariades, and R.S. Porter, Eds., Marcel Dekker Inc. (1988), New York
13. Ehrenstein, G.W., Faserverbundkunststoffe, Carl Hanser Verlag (1992), München
14. Domininghaus, H., *Plastics for Engineers*, Hanser Publishers (1993), Munich

2 Mechanical Behavior of Polymers

The mechanical properties of a polymeric component are dominated by its viscoelasticity. This is reflected by the time-dependency of the mechanical response of a component during loading. Hence, a polymer behaves differently if subjected to short term or long term loads. This chapter briefly explains polymer viscoelasticity and covers the short and long term mechanical behavior of polymers.

2.1 Viscoelastic Behavior of Polymers

A polymer, at a specific temperature and molecular weight, may behave as a liquid or a solid depending on the speed (time scale) at which its molecules deform. This behavior, which ranges between liquid and solid, is generally referred to as the viscoelastic behavior or material response. This discussion is limited to *linear viscoelasticity*, which is valid for polymer systems undergoing *small or slow deformations*. *Non-linear viscoelasticity* is required when modeling *large rapid deformations,* such as those encountered in flowing polymer melts.

In linear viscoelasticity, the *stress relaxation test* is often used, along with the *time-temperature superposition principle* and the *Boltzmann superposition principle*, to explain the behavior of polymeric materials during deformation.

2.1.1 Stress Relaxation

In a stress relaxation test, a polymer specimen is suddenly deformed a fixed amount, ε_0, and the stress required to hold that amount of deformation is recorded over time. This test is cumbersome to perform, so the design engineer and the material scientist have tended to ignore it. In fact, the standard relaxation test, ASTM D2991, was recently dropped by ASTM. Rheologists and scientists, however, have consistently used the stress relaxation test to interpret the viscoelastic behavior of polymers.

Figure 2.1 [1] presents the stress relaxation modulus measured for polyisobutylene* at various temperatures. Here, the stress relaxation modulus is defined by

$$E_r(t) = \frac{\sigma(t)}{\varepsilon_0} \tag{2.1}$$

where ε_0 is the applied strain and $\sigma(t)$ the stress being measured. From the test results, stress relaxation is clearly time and temperature dependent, especially around the glass transition temperature where the curve is steepest. For the polyisobutylene in Fig. 2.1, the glass transition temperature is about -70 °C. The measurements were completed in an experimental time window between a few seconds and one day. The tests performed at

* Better known as the matrix material for chewing gum.

EG_000216527

ClearCorrect Exhibit 1038, Page 18 of 125

lower temperatures were used to record the initial relaxation while these at higher temperatures only captured the end of relaxation of the rapidly decaying stresses.

The time it takes for the imposed stresses to relax is governed by the relaxation time, λ. High temperatures lead to small molecular relaxation times and low temperatures lead to materials with long relaxation times. When changing temperature, the shape of relaxation test results remains the same, except for a horizontal shift to the left or right, representing lower or higher response times, respectively.

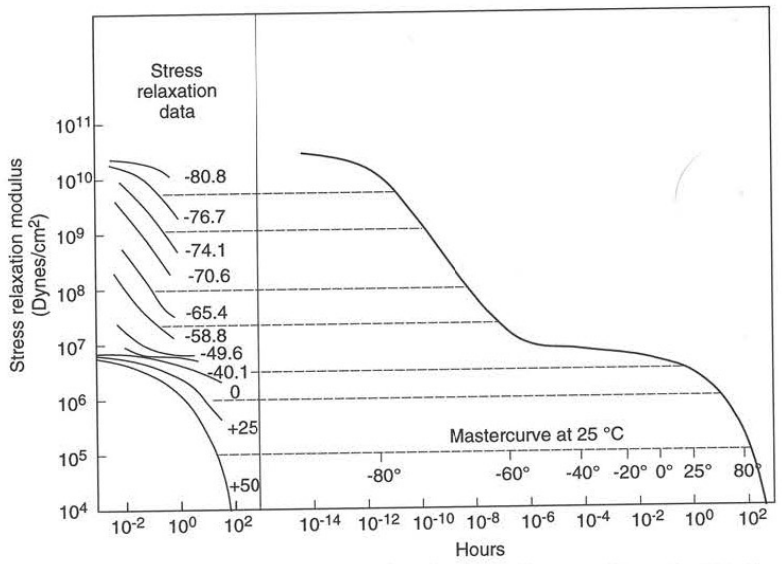


Figure 2.1 Relaxation modulus curves for polyisobutylene and corresponding master curve at 25 °C

2.1.2 Time-Temperature Superposition

The time-temperature equivalence seen in stress relaxation test results can be used to reduce data at various temperatures to one general *master curve* for a reference temperature, T. To generate a master curve at any reference temperature, the curves shown on the left of Fig. 2.1 must be shifted horizontally, holding the reference curve fixed. The master curve for the data in Fig. 2.1 is on the right of the figure. Each curve was shifted horizontally until the ends of all the curves superposed. The amount that each curve was shifted can be plotted with respect to the temperature difference taken from the reference temperature. For the data in Fig. 2.1, the shift factor is shown in Fig. 2.2 .

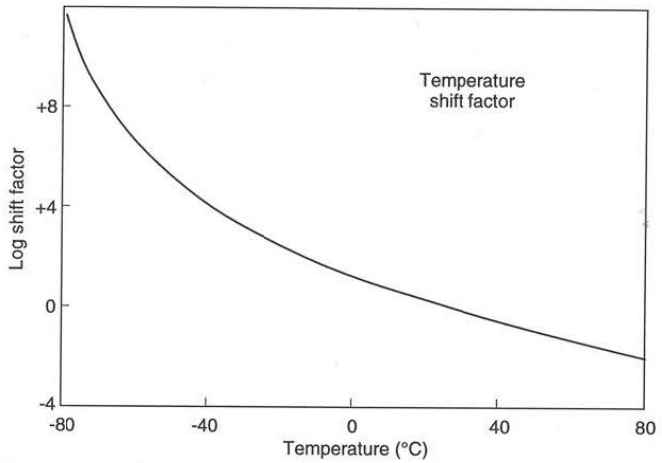


Figure 2.2 Shift factor as a function of temperature used to generate the master curve plotted in Fig. 2.1

WLF EQUATION [2]

The amount relaxation curves must be shifted in the time axis to line-up with the master curve at a reference temperarture is represented by

$$\log t - \log t_{ref} = \log\left(\frac{t}{t_{ref}}\right) = \log a_T \qquad (2.2)$$

Although the results in Figure 2.2 where shifted to a reference temperature of 298 K (25 °C), Williams, Landel and Ferry [2] chose T_{ref} = 243 K for

$$\log_{10} a_T = \frac{-8.86(T - T_{ref})}{101.6 + T - T_{ref}} \qquad (2.3)$$

which holds for nearly all amorphous polymers if the chosen reference temperature is 45 K above the glass transition temperature. In general, the horizontal shift, log a_T, between the relaxation responses at various temperatures to a reference temperature can be computed using the well known Williams-Landel-Ferry [2] (WLF) equation. The WLF equation is

$$\log_{10} a_T = -\frac{C_1(T - T_{ref})}{C_2 + (T - T_{ref})} \qquad (2.4)$$

where C_1 and C_2 are material dependent constants. It has been shown that with C_1 = 17.44 and C_2 = 51.6, Eq. 2.4 fits well for a wide variety of polymers as long as the glass transition temperature is chosen as the reference temperature. These values for C_1 and C_2 are often referred to as

EG_000216528

ClearCorrect Exhibit 1038, Page 19 of 125

universal constants. Often, the WLF equation must be adjusted until it fits the experimental data. Master curves of stress relaxation tests are important since the polymer's behavior can be traced over much greater periods than those that can be determined experimentally.

BOLTZMANN SUPERPOSITION PRINCIPLE

In addition to the *time-temperature superposition principle* (WLF), the *Boltzmann suprposition principle* is of extreme importance in the theory of linear viscoelasticity. The Boltzmann superposition principle states that the deformation of a polymer component is the sum or superposition of all strains that result from various loads acting on the part at different times. This means that the response of a material to a specific load is independent of pre-existing loads. Hence, we can compute the deformation of a polymer specimen upon which several loads act at different points in time by simply adding all strain responses.

2.2 The Short-Term Tensile Test

The most commonly used mechanical test is the short-term stress-strain tensile test. Stress-strain curves for selected polymers are displayed in Fig. 2.3 [3]. For comparison, the figure also presents stress-strain curves for copper and steel. Although they have much lower tensile strengths, many engineering polymers exhibit much higher strains at break than metals.

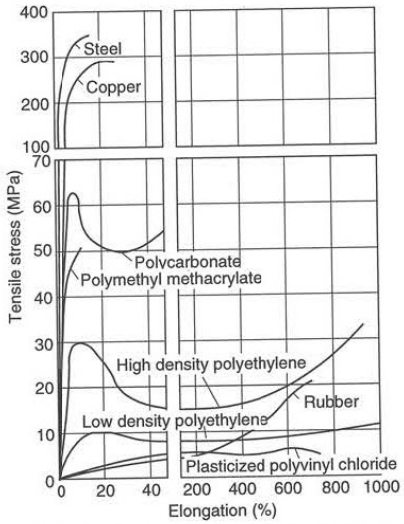


Figure 2.3 Tensile stress-strain curves for several materials

The next two sections discuss the short-term tensile test for cross-linked elastomers and thermoplastic polymers separately. The main reason for separating these two polymers is

that the deformation of a crosslinked elastomer and an uncrosslinked thermoplastic differ greatly. The deformation in a crosslinked polymer is generally reversible, while the deformation in typical uncross-linked polymers is associated with molecular chain relaxation, making the process time dependent, and irreversible.

2.2.1 Elastomers

The main feature of cross-linked elastomeric materials is that they can undergo large, reversible deformations. This is because the curled polymer chains stretch during deformation but are hindered from sliding past each other by the crosslinks between the molecules. Once a load is released, most molecules recoil. As an elastomeric polymer component is deformed, the slope in the stress-strain curves drops significantly because the uncurled molecules provide less resistance and entanglement, allowing them to move more freely. Eventually, at deformations of about 400%, the slope starts to increase because the polymer chains are fully stretched. This stretch is followed by polymer chain breakage or crystallization, ending with the fracture of the component. Stress-deformation curves for natural rubber (NR) [4] and a rubber compound [5] composed of 70 parts of styrene-butadiene-rubber (SBR) and 30 parts of natural rubber are shown in Fig. 2.4.

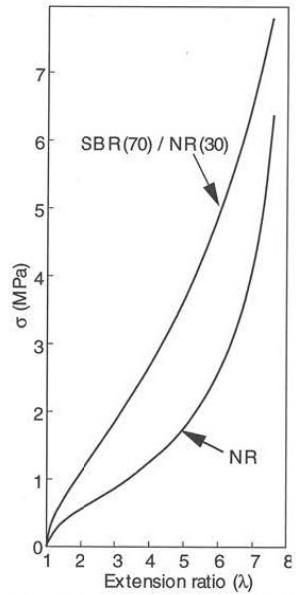


Figure 2.4 Experimental stress-extension curves for NR and a SBR/NR compound

Because of the large deformations, typically several hundred percent, the stress-strain data is usually expressed in terms of the extension ratio, λ, defined by

EG_000216529

ClearCorrect Exhibit 1038, Page 20 of 125

$$\lambda = \frac{L}{L_0} \tag{2.5}$$

where L and L_0 are the instantaneous and initial lengths of the specimen, respectively.

RUBBER ELASTICITY

For a component in uniaxial extension, or compression, the stress can be computed as

$$\sigma = G_0\left(\lambda - \frac{1}{\lambda^2}\right) \tag{2.6}$$

where G_0 is the shear modulus at zero extension, which for rubbers can be approximated by

$$G_0 = \frac{E_0}{3} \tag{2.7}$$

with E_0 as the elastic tensile modulus at zero extension. The model agrees with expriments up to about 50% extension ($\lambda = 1.5$). For compression, the model agrees much better with experiments, as shown for natural rubber in Fig. 2.5 [4]. Fortunately, rubber products are rarely deformed more than 25% in compression or tension, allowing the use of the above model.

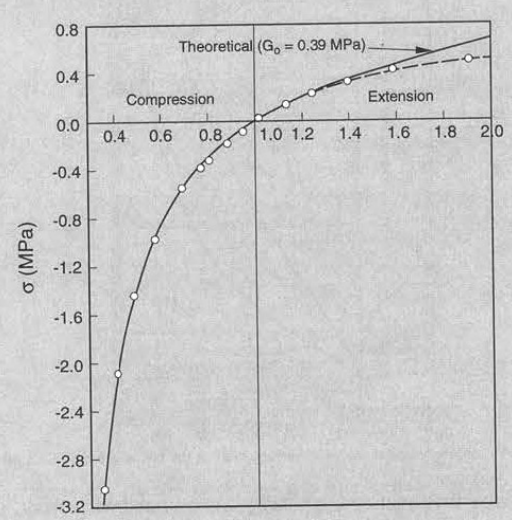


Figure 2.5 Experimental and theoretical stress-extension and compression curves for natural rubber

The corresponding model for equibiaxial extension (inflation) of thin sheets is:

$$\sigma = G_0\left(\lambda^2 - \frac{1}{\lambda^4}\right) \tag{2.8}$$

2.2.2 Thermoplastic Polymers

Of all the mechanical tests done on thermoplastic polymers, the tensile test is the least understood, and the results are often misinterpreted and misused. Since the test was inherited from other materials that have linear elastic stress-strain responses, it is often inappropriate for testing polymers.

A typical test performed on PMMA at various strain rates at room temperature is shown in Fig. 2.6. The increased curvature in the results with slow elongational speeds suggests that stress relaxation plays a significant role during the test. Here, the high rates of deformation reduce the loading time, allowing higher stress to build-up during the test.

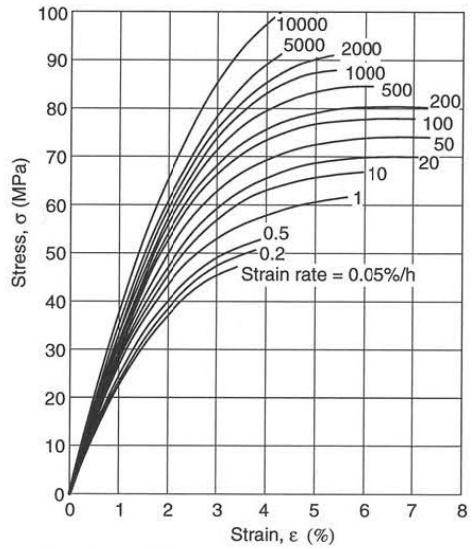


Figure 2.6 Stress-strain behavior of PMMA at various strain rates

MECHANICAL BEHAVIOR OF FILLED POLYMERS

The stiffness and strength of polymers and rubbers is increased by filling them with solid particles such as calcium carbonate and carbon black. The most common expression for describing the effect of carbon black content on the modulus of rubber was originally derived by Guth and Simha [7] for the viscosity of particle suspensions, and later used by Guth [8] to

EG_000216530

ClearCorrect Exhibit 1038, Page 21 of 125

predict the modulus of filled polymers. The Guth equation can be written as

$$\frac{G_f}{G_0} = 1 + 2.5\phi + 14.1\phi^2 \tag{2.9}$$

where G_f is the shear modulus of the filled material and ϕ is the volume fraction of particulate filler. The above expression is compared to experiments [9, 10] in Fig. 2.7.

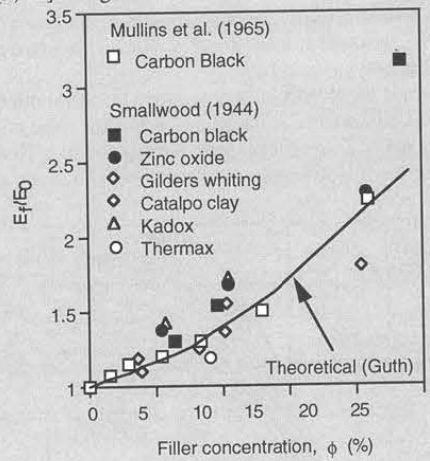


Figure 2.7 Modulus ratio of filled to unfilled natural rubber

2.3 Long-Term Tests

The *stress relaxation* and the *creep* test are well-known long-term tests. The stress relaxation test is difficult to perform and is, therefore, often approximated by data acquired through the more commonly used creep test. The stress relaxation of a polymer is often considered the inverse of creep.

The creep test, which can be performed either in shear, compression, or tension, measures the flow of a polymer component under a constant load. It is a common test that measures the strain, ε, as a function of stress, time, and temperature. Standard creep tests such as DIN 53 444 and ASTM D2990 can be used. Creep tests are performed at a constant temperature, using a range of applied stress, as shown in Fig. 2.8 [11], where the creep responses of a polypropylene copolymer are presented for a range of stresses in a graph with a log scale for time. If plotting creep data in a log-log graph, in the majority of the cases, the creep curves reduce to straight lines. Hence, the creep behavior of most polymers can be approximated with a power law:

$$\varepsilon(t) = M(\sigma,T)t^n \tag{2.10}$$

where M and n are material dependent properties.

As for the stress relaxation test, the creep behavior of a polymer depends heavily on the material temperature during testing, with the highest rates of deformation near the glass transition temperature.

Creep data is often presented in terms of the creep modulus, E_c, defined by

$$E_c = \frac{\sigma_0}{\varepsilon(t)}. \tag{2.11}$$

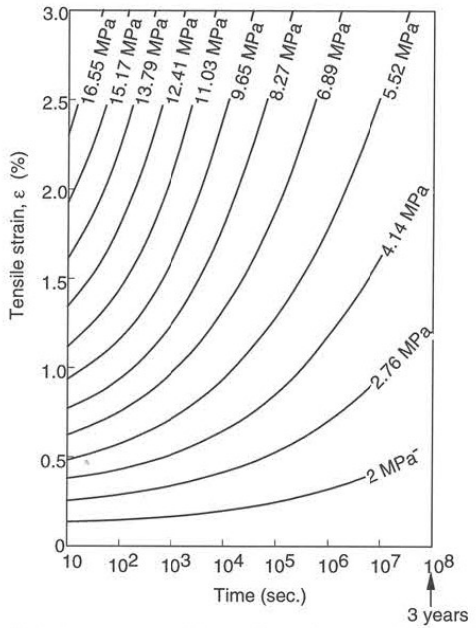


Figure 2.8 Creep response of a propylene-ethylene copolymer at 20 °C

2.3.1 Isochronous and Isometric Creep Plots

Typical creep test data, shown in Fig. 2.8, can be manipulated to be displayed as short-term stress-strain tests or as stress relaxation tests. These manipulated creep curves are called *isochronous* and *isometric* graphs.

An isochronous plot of the creep data is generated by cutting sections through the creep curves at constant times and plotting the stress as a function of strain. The isochronous curves of the creep data in Fig. 2.8 are in Fig. 2.9 [11]. Similar curves can also be generated by performing a series of *short creep tests*, where a specimen is loaded at a specific stress for a short period, typically around 100 seconds [12]. The load is then removed, and the specimen relaxes for a period of at least four times the loading interval. The specimen is then reloaded at a different stress, and the test is repeated until there are sufficient points for an isochronous graph. This procedure is more expedient than the

EG_000216531

ClearCorrect Exhibit 1038, Page 22 of 125

regular creep test and is often used to predict the short-term behavior of polymers. However, it should be pointed out that the short-term tests described in section 2.2.2 are more accurate, quicker, and less expensive to run.

The isometric or "equal size" plots of the creep data are generated by taking constant strain sections of the creep curves and by plotting the stress versus time. Isometric curves of the polypropylene creep data in Fig. 2.8 are in Fig. 2.10 [11]. This plot resembles the stress relaxation test results and is often used similarly. When we divide the stress axis by the strain, we can also plot the modulus versus time.

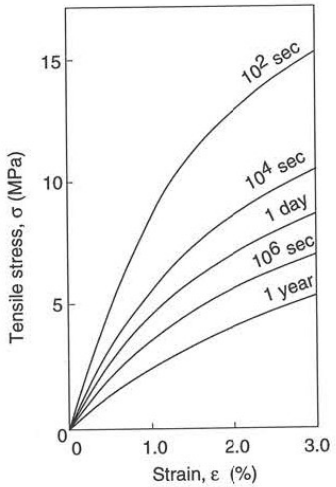


Figure 2.9 Isochronous stress-strain curves for the creep responses in Fig. 2.8

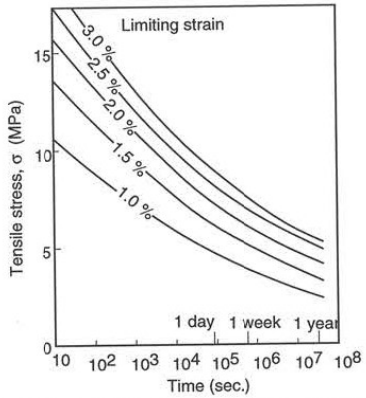


Figure 2.10 Isometric stress-time curves for the creep responses in Fig. 2.8

2.3.2 Creep Rupture

A creeping polymer component eventually undergoes catastrophic failure, generally called creep rupture or static fatigue. The standard test for creep rupture is the same as the creep test discussed earlier. Results from creep rupture tests are usually graphs of applied stress versus the logarithm of time to rupture. An example of a creep rupture test that ran for 10 years is shown in Fig. 2.11 [13,14]. These tests were done between 1958 and 1968 at Hoechst AG, Germany. Here, the creep rupture of HDPE pipes under internal pressures was tested at different temperatures. Two general regions with different slopes become obvious in the plots. The curves to the left of the knee correspond to ductile failure, whereas those to the right correspond to brittle failure. Generating a graph such as the one presented in Fig. 2.11 is lengthy, taking several years of testing. Once the steeper slope, typical of brittle fracture, has been reached, extrapolation with some confidence can be used to estimate future creep rupture times.

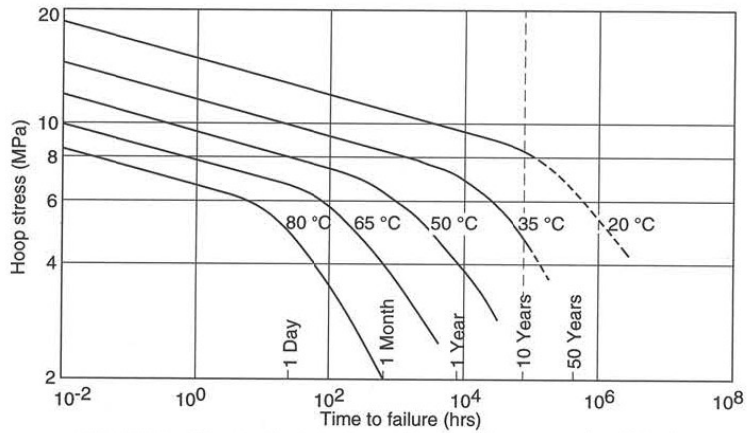


Figure 2.11 Creep rupture behavior as a function of temperature for a HDPE

2.4 Dynamic Mechanical Tests

The sinusoidal oscillatory test, also called the dynamic-mechanical-analysis (DMA) test, is one of the most useful mechanical tests for polymers. Here, a specimen is excited with a low frequency stress input which is recorded along with the strain response. The shapes of the test specimen and the testing procedure vary significantly from test to test. The various tests and their corresponding specimen shapes are described by ASTM D4065 and the terminology is described by ASTM D4092. The typical responses measured in these dynamic tests are a storage modulus, G', and a loss modulus, G". The storage modulus is related to the elastic modulus of the polymer at the loading frequency and the

EG_000216532

ClearCorrect Exhibit 1038, Page 23 of 125

loss modulus to the damping or dissipative component observed during loading. The loss modulus can also be written in terms of loss tangent (tanδ) or logarithmic decrement, Δ. The latter is related to the damping of a freely oscillating specimen.

Figure 2.12 [3] shows the elastic shear modulus and the logarthmic decrement or loss factor for various polypropylene grades. Here, the glass transition temperatures and the melting temperatures can be seen for the various polypropylene grades. The vertical scale in plots such as in Fig. 2.12 is usually logarithmic. However, a linear scale better describes the mechanical behavior of polymers in design aspects. Figure 2.13 [3] presents the elastic shear modulus versus temperature on a linear scale for several thermoplastic polymers.

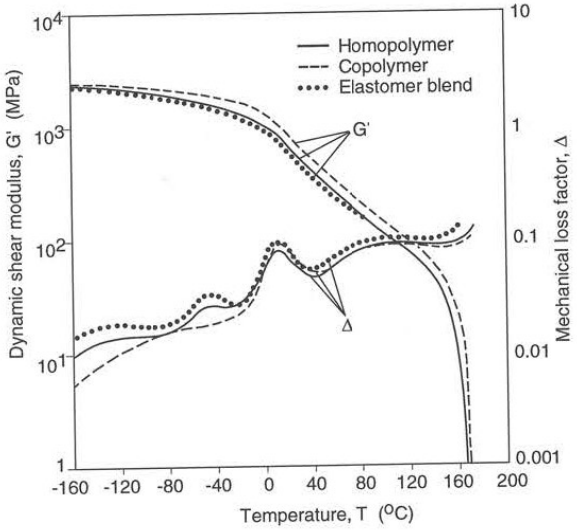


Figure 2.12 Elastic shear modulus and loss tangent for various polypropylene grades

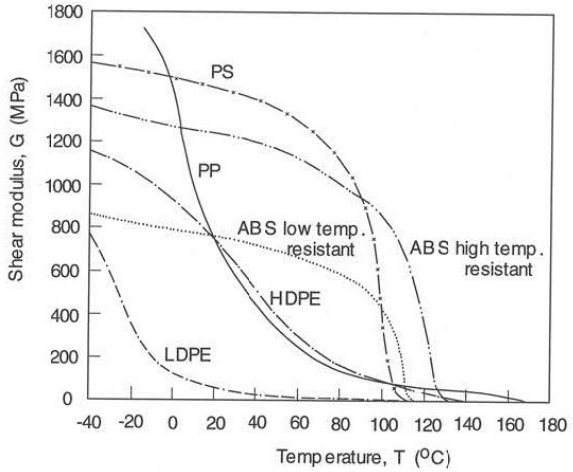


Figure 2.13 Elastic shear modulus for various polymers

SINUSOIDAL OSCILATORY TEST

If the test specimen in a sinusoidal oscillatory test is linearly elastic, the stress input and strain response would be in phase with the stress:

$$\tau(t) = \tau_0 \cos \omega t \tag{2.12}$$

$$\gamma(t) = \gamma_0 \cos \omega t \tag{2.13}$$

For an ideally viscous test specimen (Newtonian), the strain response lags $\frac{\pi}{2}$ radians behind the stress input:

$$\tau(t) = \tau_0 \cos \omega t \tag{2.14}$$

$$\gamma(t) = \gamma_0 \cos\left(\omega t - \frac{\pi}{2}\right) \tag{2.15}$$

Polymers behave somewhere in between these cases and their response is described by:

$$\tau(t) = \tau_0 \cos \omega t \text{ and} \tag{2.16}$$

$$\gamma(t) = \gamma_0 \cos (\omega t - \delta) \tag{2.17}$$

EG_000216533

ClearCorrect Exhibit 1038, Page 24 of 125

The shear modulus is complex

$$G^* = \frac{\tau(t)}{\gamma(t)} = \frac{\tau_0 e^{i\delta}}{\gamma_0} = \frac{\tau_0}{\gamma_0}(\cos\delta + \mathbf{i}\sin\delta) = G' + G'' \qquad (2.18)$$

where G' is usually called the *storage modulus* and G" is the *loss modulus* The ratio of loss modulus to storage modulus is called the *loss tangent:*

$$\tan\delta = \frac{G''}{G'} \qquad (2.19)$$

Although the elastic shear modulus G' and the loss modulus, G", are sufficient to characterize a material, one can also compute the logarithmic decrement, Δ, or loss factor by using

$$\Delta = \left(\frac{G''\pi}{G'}\right) \qquad (2.20)$$

The logarithmic decrement can also be written in terms of *loss tangent* tanδ, where δ is the mechanical loss angle. The loss tangent is then

$$\tan\delta = \frac{G''}{G'} = \frac{\Delta}{\pi} \qquad (2.21)$$

2.5 Mechanical Behavior of Filled and Reinforced Polymers

Fillers are materials intentionally inserted in polymers to make them stronger, lighter, electrically conductive or less expensive. Any filler affects the mechanical behavior of a polymetric material. For example, long fibers make the polymer stiffer but usually denser, whereas foaming makes it more compliant and much lighter. On the other hand, a filler such as calcium carbonate decreases the polymer's toughness, while making it considerably cheaper to produce.

Reinforced plastics are matrix polymers whose properties have been enhanced by introducing a reinforcement (fibers) of higher stiffness and strength. Such a material is usually called a *fiber reinforced polymer* (FRP) or a *fiber reinforced composite* (FRC). The purpose of introducing a fiber into a matrix is to transfer the load from the weaker material to the stronger one. This load transfer occurs over the length of the fiber as shown in Fig. 2.14.

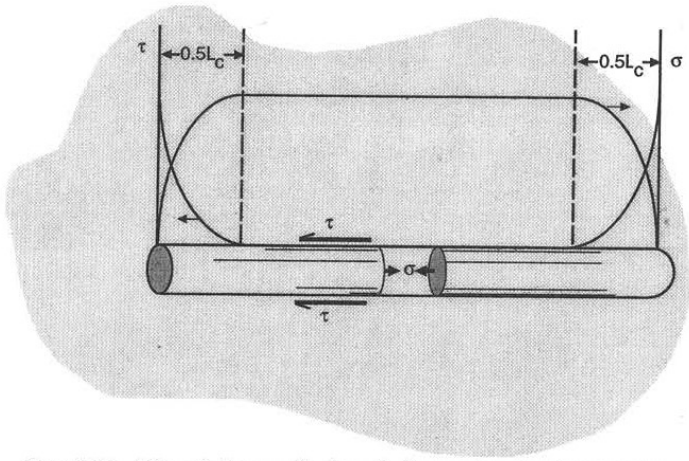


Figure 2.14 Schematic diagram of load transfer from matrix to fiber in a composite

The length to complete the load transfer from the matrix to the fiber, without fiber or matrix fracture, is usually called the critical length, L_c. For the specific case where there is perfect adhesion between fiber and matrix, experimental evidence suggests that aspect ratios of 100 or higher are required for maximum strength [15]. If composites have fibers that are shorter than their critical length they are referred to as *short fiber composites*. If the fibers are longer, they are called *long fiber composites* [16].

PROPERTIES OF FIBER REINFORCED COMPOSITES

Halpin and Tsai [17] developed a widely used model to predict the mechanical properties of aligned fiber reinforced composite laminates. With the notation in Fig. 2.15, where f and m represent the fiber and matrix, respectively; L the fiber length; D the fiber diameter; ϕ the volume fiber fraction, the longitudinal (L) and transverse (T) properties can be predicted using

$$E_L = E_m\left(\frac{1+\xi\eta\phi}{1-\eta\phi}\right) \qquad (2.22)$$

$$E_T = E_m\left(\frac{1+\eta\phi}{1-\eta\phi}\right) \qquad (2.23)$$

EG_000216534

ClearCorrect Exhibit 1038, Page 25 of 125

$$G_{LT} = G_m\left(\frac{1+\lambda\phi}{1-\lambda\phi}\right) = G_m\frac{v_{LT}}{v_m} \tag{2.24}$$

where,

$$\eta = \frac{\left(\frac{E_f}{E_m} - 1\right)}{\left(\frac{E_f}{E_m} + \xi\right)} \tag{2.25}$$

$$\lambda = \frac{\left(\frac{G_f}{G_m} - 1\right)}{\left(\frac{G_f}{G_m} + 1\right)} \tag{2.26}$$

$$\xi = 2\left(\frac{L}{D}\right) \tag{2.27}$$

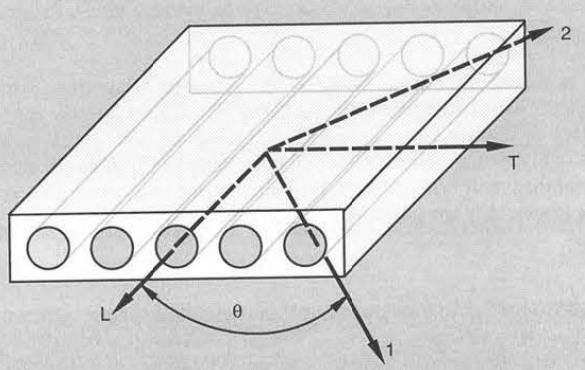


Figure 2.15 Schematic diagram of unidirectional, continuous fiber reinforced laminated structure

Most models accurately predict the longitudinal modulus as shown in Fig. 2.16 [18]. However, differences do exist between models when predicting the transverse modulus, as shown in Fig. 2.17 [18].

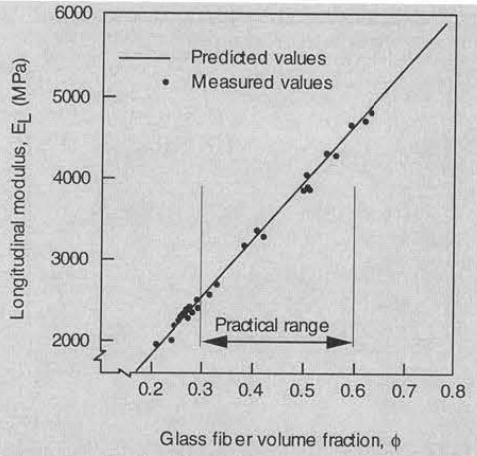


Figure 2.16 Measured and predicted longitudinal modulus for an unsaturated polyester/aligned glass fiber composite laminate as a function of volume fraction of glass content

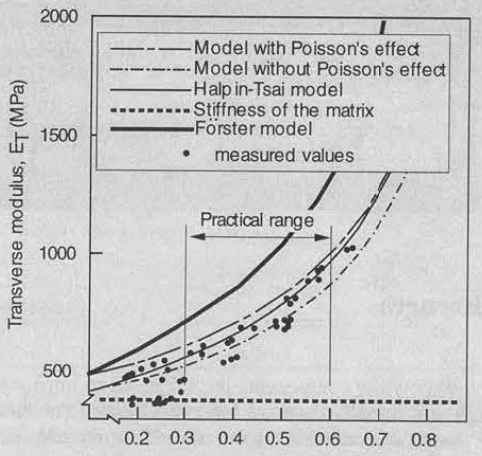


Figure 2.17 Measured and predicted transverse modulus for an unsaturated polyester/aligned glass fiber composite laminate as a function of volume fraction of glass content

Figure 2.18 [19] shows how the stiffness decreases as one rotates away from the longitudinal axis for an aligned fiber reinforced composite with different volume fraction fiber content.

EG_000216535

ClearCorrect Exhibit 1038, Page 26 of 125

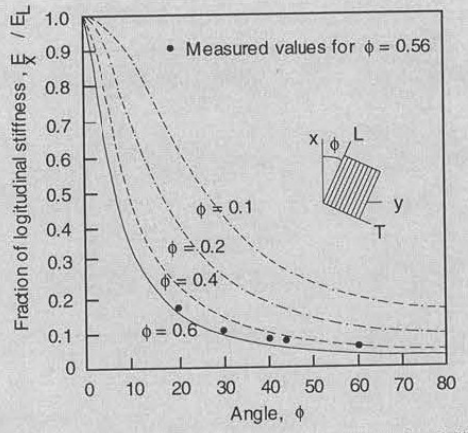


Figure 2.18 Measured and predicted elastic modulus in a uniderectional fiber reinforced laminate as a function of angle between loading and fiber direction

For high volume fraction fiber contents, only a slight misalignment of the fibers from the loading direction results in drastic property reductions.

The stiffness in a long fiber reinforced composite with a random planar orientation, such as encountered in sheet molding compound (SMC) charges, can be estimated using

$$E_{11} = E_{22} = E_{random} = \left[\frac{3}{8}\frac{1}{E_L} + \frac{3}{8}\frac{1}{E_T} - \frac{2}{8}\frac{\nu_{LT}}{E_L} + \frac{1}{8}\frac{1}{G_{LT}} \right]^{-1} \qquad (2.28)$$

2.6 Impact Strength

In practice, nearly all polymer components are subjected to impact loads. Since many polymers are tough and ductile, they are often well suited for this type of loading. However, under specific conditions even the most ductile materials, such as polypropylene, can fail in a brittle manner at low strains. These types of failure are prone to occur at low temperatures during high deformation rates.

According to several researchers [20, 21], a significantly high rate of deformation leads to complete embrittlement of polymers resulting in a lower threshold of elongation at break. Menges and Boden designed a special high speed elongational testing device to measure the minimum work required to break specimens. The minimum strain, ε_{min}, which can be measured with such a device, is a safe value to use in design calculations. One should always assume that if this minimum strain is exceeded anywhere in the component, initial fracture has already occurred. Table 2.1 [22, 23] presents minimum elongation at break values for selected thermoplastics on impact loading.

Table 2.1 Minimum Elongation at Break on Impact Loading

Polymer	ε_{min} (%)
HMW–PMMA	2.2
PA6 + 25% SFR	1.8
PP	1.8
uPVC	2.0
POM	4.0
PC + 20% SFR	4.0
PC	6.0

On the other hand, the stiffness and the stress at break of the material under consideration increases with the rate of deformation. Table 2.2 [22] presents data of the stress at break, σ_{min}, for selected thermoplastics on impact loading. This stress corresponds to the point where the minimum elongation at break has just been reached.

Table 2.2 Minimum Stress at Break on Impact Loading

Polymer	σ_{min} (MPa)
HMW-PMMA	135
PA6 + 25% Short fiber reinforced (SFR)	175
uPVC	125
POM	>130
PC + 20% SFR	>110
PC	>70

Figure 2.19 summarizes the stress-strain and fracture behavior of a HMW-PMMA tested at various rates of deformation. The area under the stress-strain curves represents the *volume-specific energy to fracture* (w). For impact, the elongation at break of 2.2% and the stress at break of 135 MPa represent a minimum of volume-specific energy because the stress increases with higher rates of deformation, but the elongation at break remains constant. Hence, if we assume a linear behavior, the *minimum volume-specific energy absorption* to fracture can be calculated using

$$w_{min} = 0.5\ \sigma_{max}\ \varepsilon_{min} \qquad (2.29)$$

EG_000216536

ClearCorrect Exhibit 1038, Page 27 of 125

If the stress-strain distribution in the polymer component is known, one can estimate the minimum energy absorption capacity using w_{min}. It can be assumed that failure occurs if w_{min} is exceeded anywhere in the loaded component. This minimum volume-specific energy absorption, w_{min}, can be used as a design parameter. It can also be used for fiber reinforced polymeric materials [24].

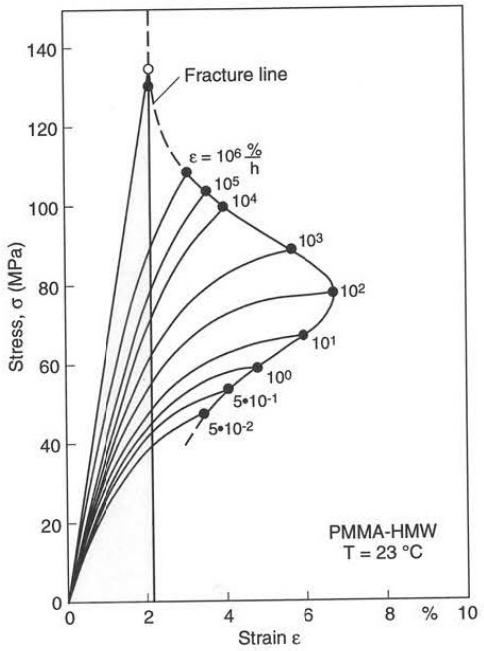


Figure 2.19 Stress-strain behavior of HMW-PMMA at various rates of deformation

2.7 Fatigue

Dynamic loading of any material that leads to failure after a certain number of cycles is called *fatigue* or *dynamic fatigue*. Dynamic fatigue is of extreme importance since a cyclic or fluctuating load causes a component to fail at much lower stresses than it does under monotonic loads.

Fatigue test results are plotted as stress amplitude versus number of cycles to failure. These graphs are usually called *S-N curves*, a term inherited from metal fatigue testing. Figure 2.20 [25] presents S-N curves for several thermoplastic and thermoset polymers tested at a 30 Hz frequency and about a zero mean stress, σ_m.

Fatigue in plastics is strongly dependent on the environment, the temperature, the frequency of loading, and surface finish. For example, bacause of surface irregularities and scratches, crack initiation at the surface is more likely in a polymer component that has been machined than in one that was injection molded. An injection molded article is formed by several layers of different orientation. In such parts, the outer layers act as a protective skin that inhibits crack initiation. In an injection molded part, cracks are more likely to initiate inside the component by defects such as weld lines and filler particles. The gate region is also a prime initiator of fatigue cracks. Corrosive environments also accelerate crack initiation and failure via fatigue.

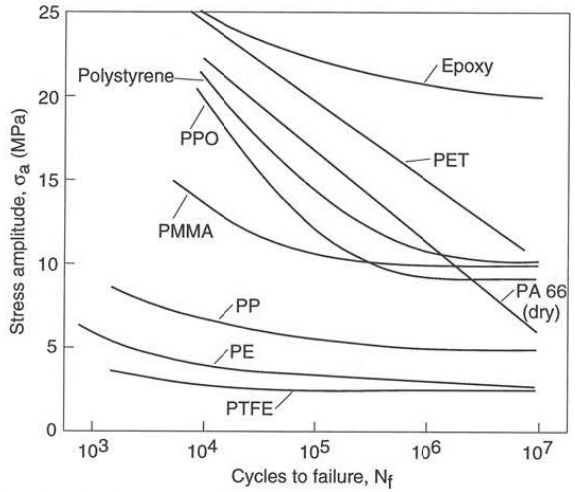


Figure 2.20 Stress-life (S-N) curves for several thermoplastic and thermoset polymers tested at a 30 Hz frequency about a zero mean stress

Temperature increases during testing is one of the main causes of failure when experimentally testing thermoplastic polymers under cyclic loads. The temperature rise during testing is caused by the combination of internal frictional or hysteretic heating and low thermal conductivity. At low frequency and stress, the temperature in the polymer specimen will rise and can eventually reach thermal equilibrium when the heat generated by hysteretic heating equals the heat removed from the specimen by conduction. As the frequency is increased, viscous heat is generated faster, causing the temperature to rise even further. After thermal equilibrium has been reached, a specimen eventually fails by conventional brittle fatigue, assuming the stress is above the endurance limit. However, if the frequency or stress level is increased even further, the temperature rises to the point

EG_000216537

ClearCorrect Exhibit 1038, Page 28 of 125

that the test specimen softens and ruptures before reaching thermal equilibrium. This mode of failure is usually referred to as *thermal fatigue.*

2.8 Weathering

When exposed to the elements, polymeric materials can exhibit environmental cracks, which lead to failure at stress levels significantly lower than those without these environments. Ultraviolet radiation, moisture, and extreme temperatures harm the mechanical properties of plastic parts.

The strength losses and discoloration from weathering are mainly attributed to the ultraviolet rays in sunlight. This can be demonstrated by plotting properties as a function of sunlight exposure instead of total time exposed. Figure 2.21 [26] is a plot of percent of initial impact strength for an ABS as a function of sunlight exposure in three different locations, Florida, Arizona, and West Virginia. The curve reveals that by "normalizing" the curves with respect to exposure to sunshine, the three different sites with three completely different weather conditions lead to the same relationship between impact strength and sunlight exposure.

The effect of weathering can often be mitigated with pigments, such as TiO_2 or carbon black, which absorb ultraviolet radiation, preventing penetration through the polymer component surface.

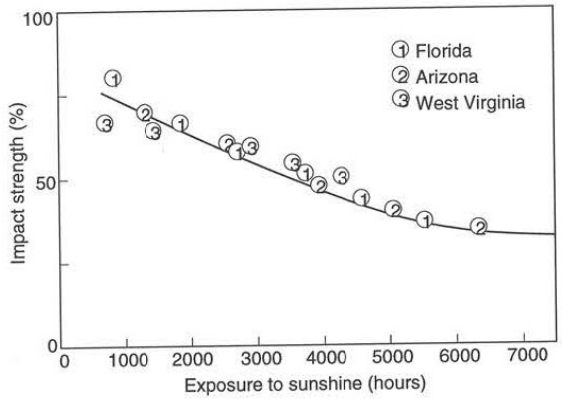


Figure 2.21 Impact strength of an ABS as a function of hours of actual sunlight exposure

Examples

2.1 For the poly-α-methylstyrene stress relaxation data in Fig.2.22 [27], create a master creep curve at T_g (204°C).

Identify the glassy, rubbery, viscous, and viscoelastic regions of the master curve. Identify each region with a spring-dashpot model diagram.

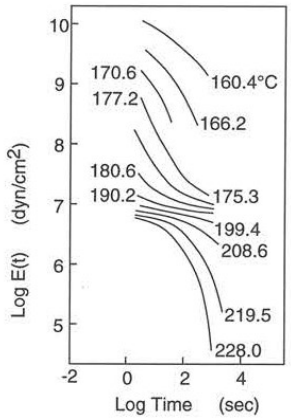


Figure 2.22 Stress relaxation data for poly-α-methylstyrene

The master creep curve for the above data is generated by sliding the individual relaxation curves horizontally until they match with their neighbors if the scale is fixed for a hypothetical curve at 204°C. Since a curve does not exist for the desired temperature, we can interpolate between 208.6°C and 199.4 °C. The resulting master curve is plotted on Fig.2.23. The amount each curve must be shifted to meet the master curve is the shift factor, Log a_T. Figure 2.24 represents the shift factor versus temperature. The solid line indicates the shift factor predicted by the WLF equation. Good agreement can be seen.

EG_000216538

ClearCorrect Exhibit 1038, Page 29 of 125

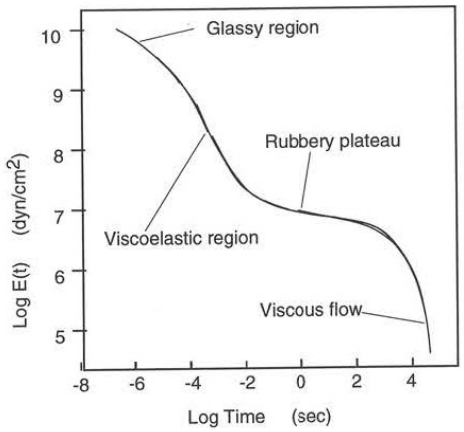


Figure 2.23 Master curve for poly-α-methylstyrene at 204°C

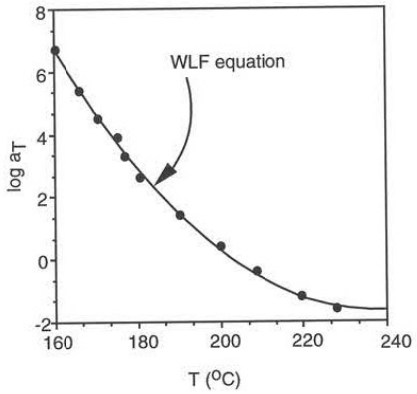


Figure 2.24 Shift factor and WLF for T_{ref}=204°C

Problems

2.1 Attached are some creep data for polystyrene at various temperatures [28]. Create a master curve at 109.8 °C by graphically sliding the curves at some temperatures horizontally until they line up.

Develop a plot of the shift factor, $\log(a_T)$ versus T, used to create your master curve. Compare your result with the WLF equation. The WLF equation is for a master curve at Tg (85 °C for this PS), but your master curve is for 109.8 °C, so be sure you make a fair comparison, such as shifting the results from the WLF equation, i.e., $(\text{Log}a_T)_{new} = \text{Log}a_T + K$.

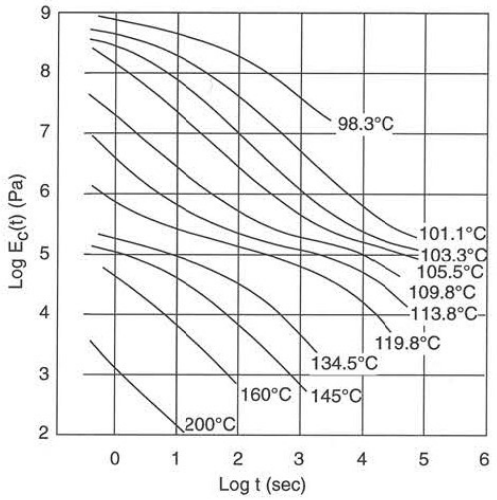


Figure 2.25 Creep modulus data for polystyrene.

2.2 Estimate the shear modulus constant, G_0, for the natural rubber (NR) and the styrene butadiene ruber-natural rubber compound (SBR/NR) presented in Fig. 2.4.

2.3 Generate 1 hour, 1 day, and 1 year isochronous (stress-strain) curves for polyacetal copolymer using the creep data presented below [3].

EG_000216539

ClearCorrect Exhibit 1038, Page 30 of 125

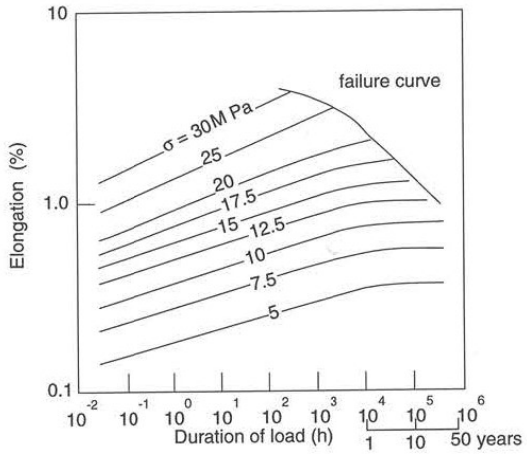


Figure 2.26 Creep data for polyacetal

2.4 What is the life expectancy of a polyacetal bracket with maximum bending stresses of 22 MPa ?

2.5 Generate a 2-year isochronous curve for the polypropylene curve presented in Fig. 2.8. Using this curve, estimate the thickness of a 50 mm diameter polypropylene pipe whose maximum allowable strain in a 2-year period should be 2%, while subjected to a 200 kPa internal pressure. Note: neglect the effect of biaxial state of stress.

2.6 Estimate the longitudinal modulus, E_L, transverse modulus, E_T, and shear modulus, G_{LT}, for a pultruded beam with unidirectional fibers. The matrix is an unsaturated polyester with E_m = 2,500 MPa and ν_m = 0.32, and the fibers are glass with E_f=73,000 MPa and ν_f = 0.25.

2.7 Estimate the planar modulus of a compression molded automotive hood with the reinforcing fibers randomly oriented in the plane of the hood. The matrix is an unsaturated polyester with E_m = 4,000 MPa and ν_m = 0.32, and the fibers are glass with E_f = 73,000 MPa and ν_f = 0.25.

2.8 The PMMA presented in Fig. 2.19 will be used for an automotive stop light and subjected to impact loading. What is the minimum volume specific energy absorbed before fracture ?

References

1. Castiff, E. and A.V.J. Tobolsky, *Colloid Sci.* (1955), *10*, 375
2. Williams, M.L., R.F. Landel, and J.D. Ferry, *J. Amer. Chem. Soc.* (1955), 77, 3701
3. Domininghaus, H., *Plastics for Engineers*, Hanser Publishers (1993), Munich
4. Treloar, L.R.G., *The Physics of Rubber Elasticity*, 3rd. Ed. (1975), Clarendon Press, Oxford
5. Courtesy ICIPC, Medellín, Colombia.
6. Williams, M.L., R.F. Landel, and J.D. Ferry, *J. Amer. Chem. Soc.* (1955), 77, 3701
7. Guth, E., and R. Simha, *Kolloid-Zeitschrift* (1936), *74*, 266
8. Guth, E., *Proceedings of the American Physical Society*, (1937): *Physical Review* (1938), *53*, 321
9. Smallwood, H.M., *J. Appl. Phys.* (1944), *15*, 758
10. Mullins, L., and N.R. Tobin, *J. Appl. Polym. Sci.* (1965), *9*, 2993
11. ASTM, Plastics (II), 08.02, ASTM (1994), Philadelphia
12. Crawford, R.J., *Plastics Engineering*, 2nd ed., 47, Pergamon Press (1987), Oxford
13. Richard, K., E. Gaube and G. Diedrich, *Kunststoffe* (1959), *49*, 516
14. Gaube, E. and H.H. Kausch, *Kunststoffe* (1973), *63*, 391
15. Nielsen, L.E., and R.F. Landel, *Mechanical Properties of Polymers and Composites*, 2nd Ed., Marcel Dekker (1994), Inc., New York
16. Krishnamachari, S.I., *Applied Stress Analysis of Plastics*, Van Nostrand Reinhold (1993), New York
17. Tsai, S.W., J.C. Halpin, and N.J. Pagano, *Composite Materials Workshop*, Technomic Publishing Co. (1968), Stamford
18. Brintrup, H., Ph.D. Thesis (1974), IKV, RWTH-Aachen, Germany
19. Menges, G., *Kunststoffverarbeitung III*, 5, Lecture notes (1987), IKV, RWTH-Aachen
20. Boyer, R.F., *Polymer Eng. Sci.* (1968), *8*, 161
21. Boden, H.E., Ph.D. Thesis (1983), IKV, RWTH-Aachen, Germany
22. Menges, G., and H.-E. Boden, *Failure of Plastics*, Chapter 9, Eds. W. Brostow, and R.D. Corneliussen, Hanser Publishers (1986), Munich
23. Andrews, E.H., *Fracture in Polymers* (1968), Oliver and Body, London
24. Rest, H., Ph.D. Thesis (1984), IKV-Aachen
25. Riddell, M.N., *Plast. Eng.*(1974), *40*, 4, 71
26. Ruhnke, G.M. and L.F. Biritz, *Kunststoffe* (1972), 62, 250
27. Fujimoto, T., M. Ozaki and M. Nagasawa, *J. Polymer Sci.* (1968., 2, 6, 129
28. Pazek, D.J., *J. Polym. Sci.*(1968), A-2, (6), 621
29. Domininghaus, H., *Plastics for Engineers*, Hanser Publishers (1993), Munich.

EG_000216540

ClearCorrect Exhibit 1038, Page 31 of 125

3 Rheology of Polymer Melts

Rheology is the science of fluid behavior during flow induced deformation. Among the variety of materials that rheologists study, polymers have been found to be the most interesting and complex. Polymer melts are shear thinning and viscoelastic and their flow properties are temperature dependent. This chapter discusses the phenomena that are typical of polymer melts and covers the basic properties used to represent the flow behavior of polymers. The chapter also introduces rheometry. For further reading on rheology of polymer melts, consult references 1 to 6.

3.1 Introduction to Rheology

Viscosity is the most widely used material parameter when determining the behavior of polymers during processing. Since the majority of polymer processes are shear rate dominated, the viscosity of the melt is commonly measured using shear deformation measurement devices. For example, the simple shear flow generated in the sliding plate rheometer [7], shown in Fig. 3.1, exhibits a deviatoric stress defined by

$$\tau_{xy} = \eta(T, \dot{\gamma})\dot{\gamma}_{xy} \tag{3.1}$$

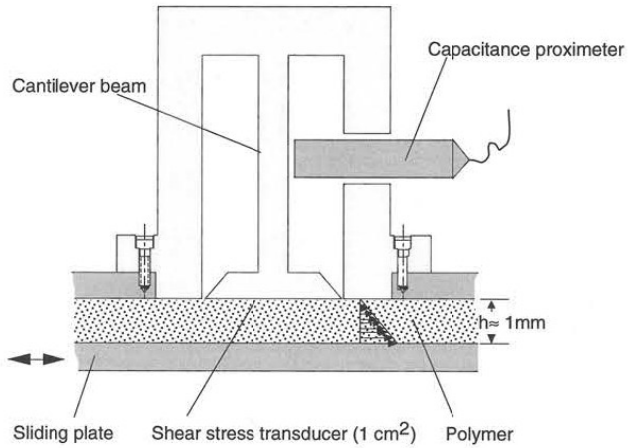


Figure 3.1. Schematic disgram of a sliding plate rheometer

ClearCorrect Exhibit 1038, Page 32 of 125

where $\eta(T,\dot{\gamma})$ is the viscosity and $\dot{\gamma}_{xy}$ the shear rate defined by v/h. For the flow in Fig. 3.1, the magnitude of the rate of deformation tensor, $\dot{\gamma}$, is $\dot{\gamma}_{xy}$. There are also polymer processes, such as blow molding, thermoforming and fiber spinning, which are dominated by either elongation or by a combination of shear and elongational deformation. In addition, some polymer melts exhibit significant elastic effects during deformation.

3.1.1 Shear Thinning Behavior of Polymers

Most polymer melts are *shear thinning fluids.* The shear thinning effect is the reduction in viscosity at high rates of deformation, such as shown in Fig. 3.2 for an LDPE resin. This phenomenon occurs because at low rates of deformation, the polymer molecules are entangled and at high rates of deformation, the molecules are stretched out and disentangled. The disentangled molecules can slide past each other more easily, thus, lowering the bulk melt viscosity.

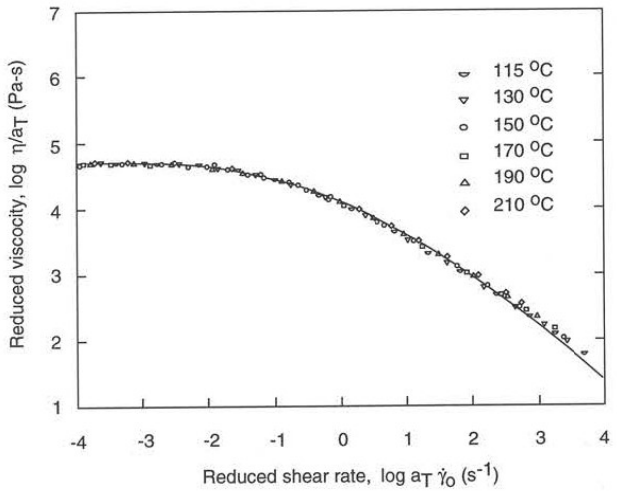


Figure 3.2 Reduced viscosity curve for an LDPE at a reference temperature of 150 °C

The power-law model proposed by Ostwald [8] and de Waale [9] is the simplest model that accurately represents the shear thinning region in the viscosity versus strain rate curve, but overshoots the Newtonian plateau at small strain rates. The power-law model is:

$$\eta = m(T)\dot{\gamma}^{n-1} \tag{3.2}$$

where m is called the *consistency index* and n the *power law index.* The consistency index may include the temperature dependence of the viscosity and can be represented as

$$m(T) = m_0 e^{-a(T-T_0)} \tag{3.3}$$

Power-law constants, as used in Eqs. (3.2) and (3.3), are presented in Table 3.1 for common thermoplastics.

Table 3.1 Power-Law Indices, Consistency Indices, and Temperature Dependence Constants for Common Thermoplastics

Polymer	m (Pa-s^n)	n	a (1/°C)	T_0(°C)
Polystyrene	2.80 x 10^4	0.28	0.025	170
High density polyethylene	2.00 x 10^4	0.41	0.002	180
Low density polyethylene	6.00 x 10^3	0.39	0.013	160
Polypropylene	7.50 x 10^3	0.38	0.004	200
Polyvinylchloride	1.70 x 10^4	0.26	0.019	180

SIMPLIFIED FLOWS COMMON IN POLYMER PROCESSING

Many polymer processing operations can be modeled using simplified geometries and material models. This section presents several isothermal flows in simple geometries using a Newtonian viscosity and a power-law viscosity as described in Eq. (3.2).

Simple shear flow (Fig. 3.3)

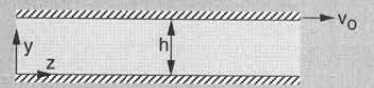


Figure 3.3 Schematic diagram of a simple shear flow

Simple shear flows are common in polymer processing, such as inside extruders as well as in certain coating flows. The flow field in simple shear is the same for all fluids and is described by

$$v_z(y) = v_0 \frac{y}{h} \tag{3.4}$$

EG_000216542

ClearCorrect Exhibit 1038, Page 33 of 125

$$Q = \frac{v_0 hW}{2} \tag{3.5}$$

Pressure flow through a slit (Fig. 3.4)

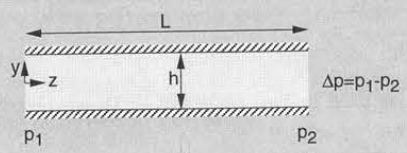


Figure 3.4 Schematic diagram of a pressure flow through a slit

The pressure flow through a slit is commonly encountered in flows through extrusion dies or inside injection molds. The Newtonian flow field is described using

$$v_z(y) = \left(\frac{h^2 \Delta p}{8\mu L}\right)\left[1 - \left(\frac{2y}{h}\right)^2\right] \tag{3.6}$$

$$Q = \frac{Wh^3 \Delta p}{12\mu L} \tag{3.7}$$

When using the power law model (Eq. (3.2)) the flow field is described by

$$v_z(y) = \left(\frac{h}{2(s+1)}\right)\left(\frac{h\Delta p}{2mL}\right)^s\left[1 - \left(\frac{2y}{h}\right)^{s+1}\right] \tag{3.8}$$

$$Q = \frac{Wh^2}{2(s+2)}\left(\frac{h\Delta p}{2mL}\right)^s \tag{3.9}$$

where s=1/n.

Pressure flow through a tube - Hagen-Poiseuille flow (Fig. 3.5)

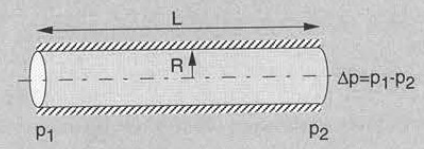


Figure 3.5 Schematic diagram of a tube flow

Pressure flow through a tube is encountered in the runner system in injection molds, in certain dies, and in the capillary rheometer. The Newtonian flow field is given by

$$v_z(r) = \frac{R^2 \Delta p}{4\mu L}\left[1 - \left(\frac{r}{R}\right)^2\right] \tag{3.10}$$

$$Q = \frac{\pi R^4 \Delta p}{8\mu L} \tag{3.11}$$

Using the power law fluid the flow field in a tube is described by

$$v_z(r) = \frac{R}{1+s}\left(\frac{R\Delta p}{2mL}\right)^s\left[1 - \left(\frac{r}{R}\right)^{s+1}\right] \tag{3.12}$$

$$Q = \left(\frac{\pi R^3}{s+3}\right)\left(\frac{R\Delta p}{2mL}\right)^s \tag{3.13}$$

Couette flow (Fig. 3.6)

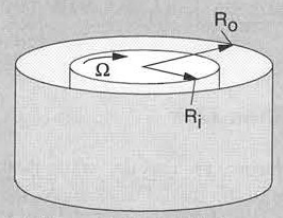


Figure 3.6 Schematic diagram of a Couette device

The Newtonian flow field in a Couette device is described by

$$v_\theta(r) = \frac{\Omega}{\kappa^2 - 1}\left(\frac{R_o^2 - r^2}{r}\right) \tag{3.14}$$

where $\kappa = R_0 / R_i$. Using the power-law model, the flow field inside a Couette device is described by

$$v_\theta(r) = \frac{\Omega}{\kappa^{2s} - 1}\left(\frac{R_o^{2s} - r^{2s}}{r^{2s-1}}\right) \tag{3.15}$$

EG_000216543

ClearCorrect Exhibit 1038, Page 34 of 125

NON-ISOTHERMAL FLOWS IN POLYMER PROCESSING

Although we simplify analyses of polymer processes by assuming isothermal conditions, most operations are non-isothermal since they include melting and viscous dissipation. Hence, the temperature of the polymer melt lies between T_g (or T_m) and the heater temperature, T_h., and often exceeds T_h due to viscous dissipation. An estimate the maximum temperature rise due to viscous heating in a simple shear flow is

$$\Delta T_{max} = \frac{\eta V_0^2}{8k} \tag{3.16}$$

To estimate if viscous dissipation is important in a polymer process, the Brinkman number, Br, is often used

$$Br = \frac{\eta V_0^2}{k(T_h - T_g)} \tag{3.17}$$

The Brinkman number is the ratio of the heat generated via viscous dissipation and the heat transport via conduction. The choice of temperature difference, e.g. $(T_h - T_g)$, depends on the type of problem being analyzed.

3.1.2 Normal Stresses in Shear Flow

The tendency of polymer molecules to "curl-up" while they are being stretched in shear flow results in normal stresses in the fluid. For example, the shear flow presented in Eq. (3.1) has measurable normal stress differences, N_1 and N_2, which are called the *first* and *second normal stress differences*, respectively. The first and second normal stress differences are material dependent and are defined by

$$N_1 = \tau_{xx} - \tau_{yy} = -\Psi_1(\dot{\gamma},T)\,\dot{\gamma}_{xy}^2 \tag{3.18}$$

$$N_2 = \tau_{yy} - \tau_{zz} = -\Psi_2(\dot{\gamma},T)\,\dot{\gamma}_{xy}^2 \tag{3.19}$$

The material functions, Ψ_1 and Ψ_2, are called the primary and secondary normal stress coefficients, and are also functions of the magnitude of the strain rate tensor and temperature. The first and second normal stress differences do not change sign when the direction of the strain rate changes. This is reflected in Eqs. (3.18) and (3.19). Figure 3.7 [10] presents the first normal stress difference coefficient for the LDPE melt of Fig. 3.2 at

a reference temperature of 150 °C. The second normal stress difference is difficult to measure and is often approximated by

$$\Psi_2(\dot{\gamma}) \approx -0.1\Psi_1(\dot{\gamma}) \tag{3.20}$$

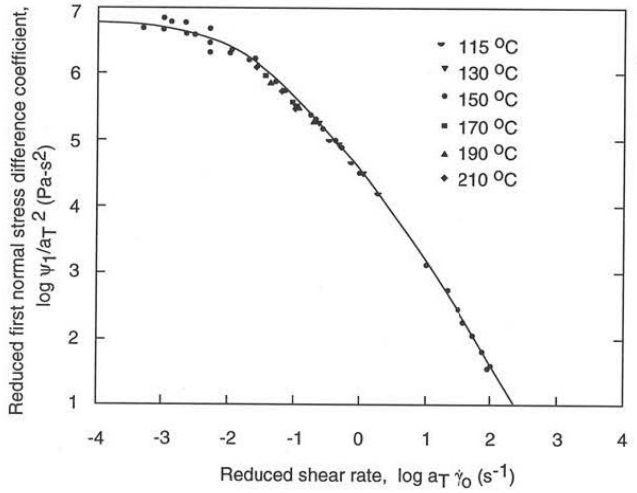


Figure 3.7 Reduced first normal stress difference coefficient for an LDPEmelt at a reference temperature of 150 °C

The normal stress differences play significant roles during processing. For example, the first normal stress difference is partly responsible for *extrudate swell* (Fig. 3.8) at the exit of the die. The second normal stress differences help diminish the eccentricity of a wire in the die during the wire coating process [11].

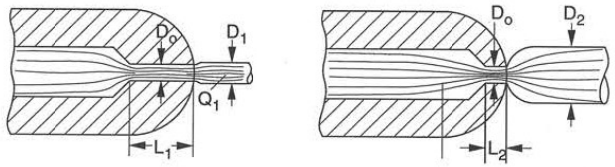


Figure 3.8 Schematic diagram of extrudate swell during extrusion

EG_000216544

ClearCorrect Exhibit 1038, Page 35 of 125

3.1.3 Deborah Number

A useful parameter for estimating the elastic effects during flow is the Deborah number:

$$De = \frac{\lambda}{t_p} \tag{3.21}$$

where λ is the relaxation time of the polymer and t_p is a characteristic process time. The characteristic process time can be defined by the ratio of characteristic die dimension and average speed through the die. A Deborah number of zero represents a viscous fluid and a Deborah number of ∞, an elastic solid. As the Deborah number exceeds one, the polymer does not have enough time to relax during the process, resulting in *extrudate swell* *, *shark skin* or even *melt fracture*.

Although many factors affect the amount of extrudate swell, fluid "memory" and normal stress effects are most significant. However, abrupt changes in boundary conditions, such as the separation point of the extrudate from the die, also play a role in the swelling or cross section reduction of the extrudate. In practice, the fluid memory contribution to die swell can be mitigated by lengthening the land length of the die. This is schematically depicted in Fig. 3.8. A long die land separates the polymer from the manifold long enough to allow it to "forget" its past shapes.

Waves in the extrudate may also appear as a result of high speeds during extrusion, where the polymer cannot relax. This phenomenon is generally called *shark skin* and is shown for an HDPE in Fig. 3.9-a [12]. Polymers can be extruded at such high speeds that an intermittent separation of melt and inner die walls occurs as shown in Fig. 3.9-b. This phenomenon is often called *stick-slip* or *spurt flow* and is attributed to high shear stresses between the polymer and the die wall. This phenomenon occurs when the shear stress is near the critical value of 0.1 MPa [13-15]. If the speed is further increased, a helical geometry is extruded as shown for a polypropylene extrudate in Fig. 3.9-c. Eventually, the speeds are so high that a chaotic pattern develops such as the one shown in Fig. 3.9-d. This well known phenomenon is called *melt fracture*. Shark skin is frequently absent, and spurt flow seems to occur only with linear polymers.

The critical shear stress has been reported to be independent of the melt temperature but inversely proportional to the weight average molecular weight [15,16]. However, Vinogradov et al. [13] presented results where the critical stress was independent of molecular weight except at low molecular weights. Dealy and co-workers [15] and Denn [17] give an extensive overview of various melt fracture phenomena. Both references are recommended.

* Newtonian fluids, which do not experience elastic or normal stress effects, also show some extrudate swell or reduction. A Newtonian fluid extruded at high shear rates reduces its cross section to 87% of the diameter of the die. This swell is the result of inertia effects caused by the rearrangement from the parabolic velocity distribution inside the die to the flat velocity distribution of the extrudate. If the polymer is extruded at very low shear rates it swells to 113% of the diameter of the die.

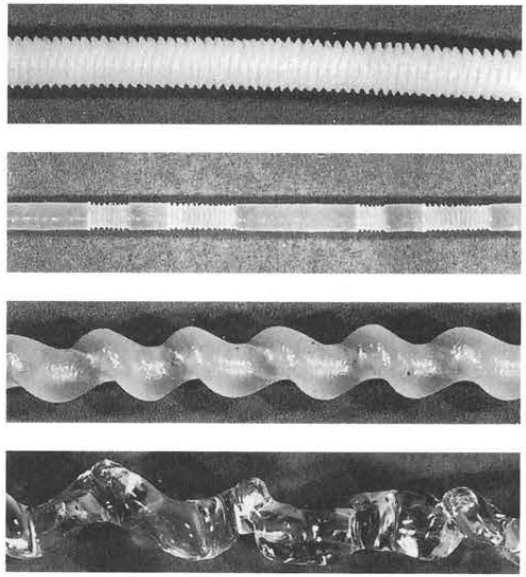


Figure 3.9 Various shapes of extrudates under melt fracture

SONG OF DEBORAH

M. Reiner is credited with naming the Deborah Number after the song of Deborah, Judges 5:5- "The mountains flowed before the Lord"(Fig. 3.10). It was first mentioned in his article "The Deborah Number" in the January 1964 issue of Physics Today.

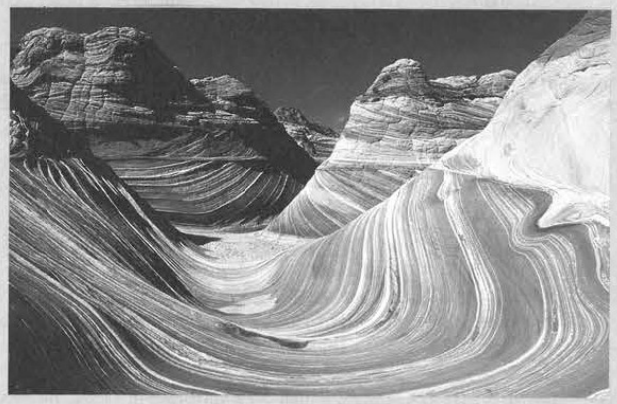


Figure. 3.10 Nestles Canyon, Arizona. Courtesy of Wolfgang Cohnen (©1997)

EG_000216545

ClearCorrect Exhibit 1038, Page 36 of 125

3.1.4 Rheology of Curing Thermosets

A curing thermoset polymer has a conversion or cure dependent viscosity that increases as the molecular weight of the reacting polymer increases. For the vinyl ester whose curing history is shown in Fig. 3.11 [19], the viscosity behaves as shown in Fig. 3.12 [17]. Hence, a complete model for viscosity of a reacting polymer must contain the effects of strain rate, $\dot{\gamma}$, temperature, T, and degree of cure, c, such as

$$\eta = \eta(\dot{\gamma}, T, c) \tag{3.22}$$

There are no generalized models that include all these variables for thermosetting polymers. However, extensive work has been done on the viscosity of polyurethanes [19, 20] used in the reaction injection molding process. An empirical relation which models the viscosity of these mixing activated polymers, given as a function of temperature and degree of cure, is written as

$$\eta = \eta_0 e^{E/RT}\left(\frac{c_g}{c_g - c}\right)^{C_1 + C_2 c} \tag{3.23}$$

where E is the activation energy of the polymer, R is the ideal gas constant, T is the temperature, c_g is the gel point , c the degree of cure, and C_1 and C_2 are constants that fit the experimental data. The gel point is the degree of cure when the molecular weight goes to infinity or when the molecules become interconnected.

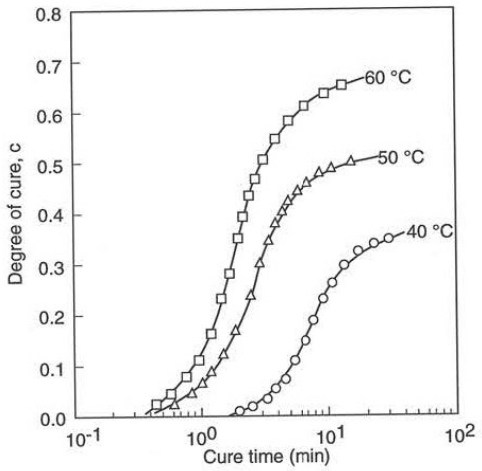


Figure 3.11 Degree of cure as a function of time for a vinyl ester at various isothermal cure temperatures

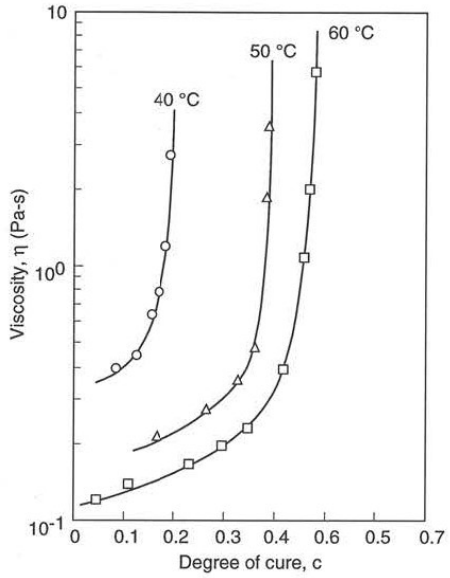


Figure 3.12 Viscosity as a function of degree of cure for a vinyl ester at various isothermal cure temperatures

3.1.5 Suspension Rheology

Particles suspended in a material, such as in filled or reinforced polymers, have a direct effect on the properties of the final article and on the viscosity during processing. The model which best fits experimental data is the one given by Guth [21]:

$$\frac{\eta f}{\eta 0} = 1 + 2.5\phi + 14.1\phi^2 \tag{3.24}$$

Figure 3.13 compares experimental data to Guth's equation. The experiments were performed on polyethylene and polystyrene containing different fill factors of spherical glass particles ranging between 36 μm and 99.8 μm in diameter. The model agrees well with the experimental data up to volume fractions of 30%.

EG_000216546

ClearCorrect Exhibit 1038, Page 37 of 125

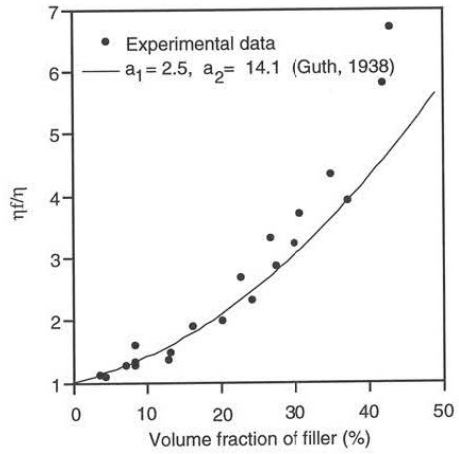


Figure 3.13 Viscosity increase as a function of volume fraction of filler for polystyrene and LDPE.

VISCOELASTIC FLOW MODELS

Viscoelasticity has already been introduced in Chapter 2 based on linear viscoelasticity. However, in polymer processing large deformations are imposed on the material, requiring the use of non-linear viscoelastic models. There are two types of general non-linear viscoelastic flow models, the differential model and the integral model.

An overview of numerical simulation of viscoelastic flow systems and an extensive literature review on the subject was given by Keunings [22], and detail on numerical implementation of viscoelastic models are given by Crochet et al. [23] and Debbaut et al. [24]. As an example of the application of differential models to predict flow of polymeric liquids, Dietsche and Dooley [25], recently evaluated the White–Metzner, the Phan-Thien Tanner-1 and the Giesekus models by comparing finite element and experimental results of the flow inside multi-layered coextrusion dies. Figure 3.14 [26] presents the progression of a matrix of dyed circular polystyrene strands flowing in an identical polystyrene matrix down a channel with a square cross section of 0.95 x 0.95 cm. The cuts in the figure are shown at intervals of 7.6 cm. The circulation pattern caused by the secondary normal stress differences inside non-circular dies were captured well by the Phan-Thien Tanner and Giesekus models but, as expected, not by the White–Metzner model. Figure 3.14 also presents flow patterns predicted by the Phan-Thien Tanner model. The shape of the circulation patterns were predicted accurately. The flow simulation of the square die predicted a velocity on the order of 10^{-5} m/s along the diagonal

of the cross section, which agreed with the experimental results. Also, Baaijens [27], recently evaluated the Phan-Thien Tanner models 1 and 2, and the Giesekus models. He compared finite element results to measured isochromatic birefringence patterns using complex experiments with polymer melts and solutions. His simulation results predicted the general shape of the measured birefringence patterns. He found that at high Deborah numbers, the Phan-Thien Tanner models converged more easily than the Giesekus model.

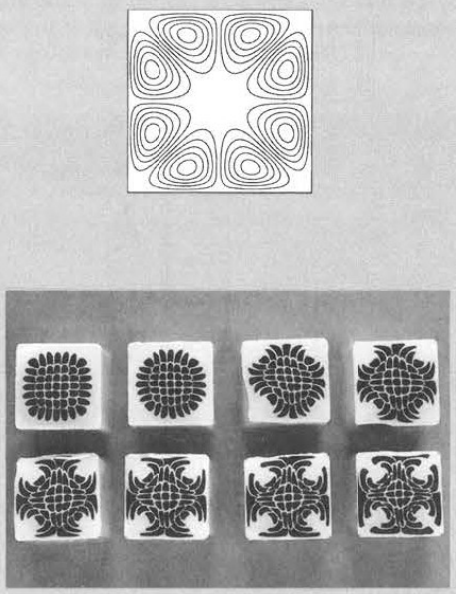


Figure 3.14 Simulated flow patterns and polystyrene strand profile progression in a square die

3.2 Rheometry

In industry, there are various ways to qualify and quantify the properties of the polymer melt. The techniques range from simple analyses for checking the consistency of the material at certain conditions, to more difficult fundamental measurements to evaluate viscosity and normal stress differences. This section includes three such techniques to give the reader a general idea of current measuring methods.

EG_000216547

ClearCorrect Exhibit 1038, Page 38 of 125

3.2.1 The Melt Flow Indexer

The melt flow indexer is often used in industry to characterize a polymer melt and as a simple and quick means of quality control. It takes a single point measurement using standard testing conditions specific to each polymer class on a ram type extruder or extrusion plastometer as shown in Fig. 3.15. The standard procedure for testing the flow rate of thermoplastics using a extrusion plastometer is described in the ASTM D1238 test [28]. During the test, a sample is heated in the barrel and extruded from a short cylindrical die using a piston actuated by a weight. The weight of the polymer in grams extruded during the 10-minute test is the melt flow index (MFI) of the polymer.

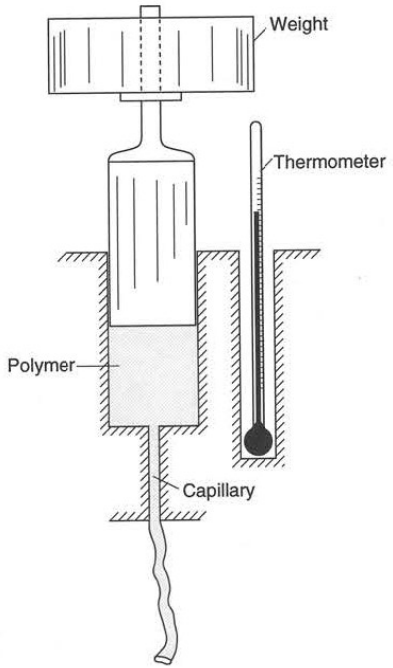


Figure 3.15 Schematic diagram of an extrusion plastometer used to measure melt flow index

3.2.2 The Capillary Viscometer

The most common and simplest device for measuring viscosity is the capillary viscometer. Its main component is a straight tube or capillary, and it was first used to measure the viscosity of water by Hagen [29] and Poiseuille [30]. A capillary rheometer has a pressure driven flow for which the shear rate is maximum at the wall and zero at the center of the flow, making it a non-homogeneous flow.

Since pressure driven viscometers employ heterogeneous flows, they can only measure steady shear functions such as viscosity, $\eta(\dot{\gamma})$. However, they are widely used because they are relatively inexpensive and simple to operate. Despite their simplicity, long capillary viscometers give the most accurate viscosity data available. Another major advantage is that the capillary rheometer has no free surfaces in the test region, unlike other types of rheometers such as the cone and plate rheometer, discussed next. When the strain rate dependent viscosity of polymer melts is measured, capillary rheometers are capable of obtaining such data at shear rates greater than 10 s^{-1}. This is important for processes with higher rates of deformation like mixing, extrusion, and injection molding. Because its design is basic and it only needs a pressure head at its entrance, the capillary rheometer can easily attach to the end of a screw- or ram-type extruder for online measurements. This makes the capillary viscometer an efficient tool for industry. The basic features of the capillary rheometer are shown in Fig. 3.16.

VISCOSITY FROM CAPILLARY VISCOMETER DATA

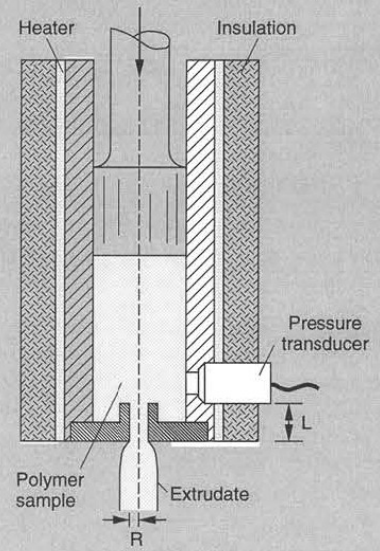


Figure 3.16 Schematic diagram of a capillary viscometer

A capillary tube of radius R and length L is connected to the bottom of a reservoir. Pressure drop and flow rate through this tube are used to determine the viscosity. At the wall, the shear stress is:

$$\tau_w = \frac{R}{2}\frac{(p_o - p_L)}{L} = \frac{R}{2}\frac{\Delta p}{L} \qquad (3.25)$$

EG_000216548

ClearCorrect Exhibit 1038, Page 39 of 125